Plasma X-ray Sources and Imaging … an ICF perspective

Advanced Summer School

9-16, Juy 2017, Anacapri, Capri, Italy

Riccardo Tommasini

Lawrence Livermore National Laboratory

LLNL-PRES-734513

This work was performed under the auspices of the U.S. Department of Energy by Lawrence Livermore National Laboratory under Contract DE-AC52-07NA27344. Lawrence Livermore National Security, LLC

Outlook

Motivation

- Our problem: probing ICF targets
- This requires the use of X-rays
- Plasmas are efficient sources of X-rays

Summary

- What is ICF
- Need to image ICF targets
- Laboratory-generated X-ray sources: laser plasma
  - Basic Plasma parameters
  - Basics of Radiation emission from laser-plasmas
- Imaging techniques
- Application of Radiography to ICF targets

Outlook

Motivation

- Our problem: probing ICF targets
- This requires the use of X-rays
- Plasmas are efficient sources of X-rays

Summary

- What is ICF
- Need to image ICF targets
- Laboratory-generated X-ray sources: laser plasma
  - Basic Plasma parameters
  - Basics of Radiation emission from laser-plasmas
- Imaging techniques
- Application of Radiography to ICF targets

Nuclear energy is released when the final reaction products have less mass/nucleon than the reacting nuclei

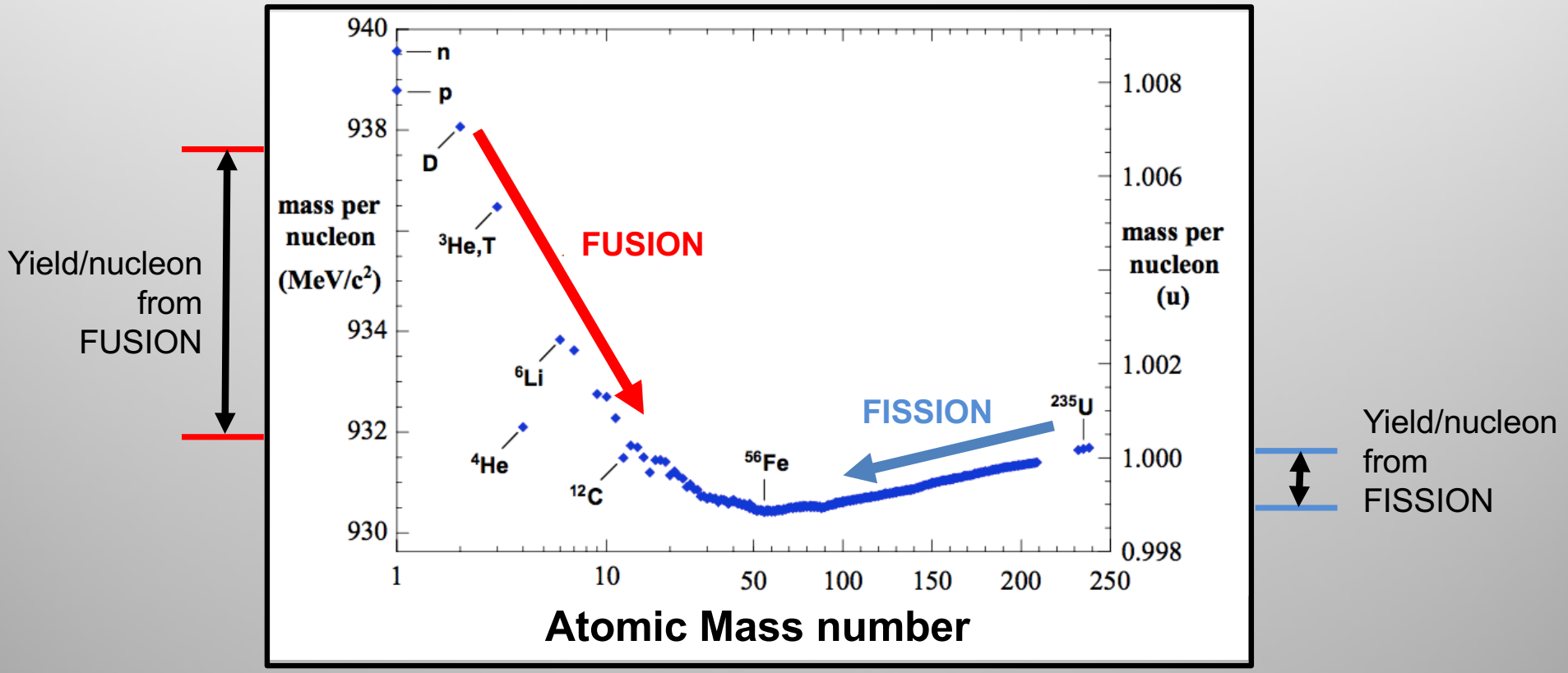

Temperatures of several keV are needed for fusion

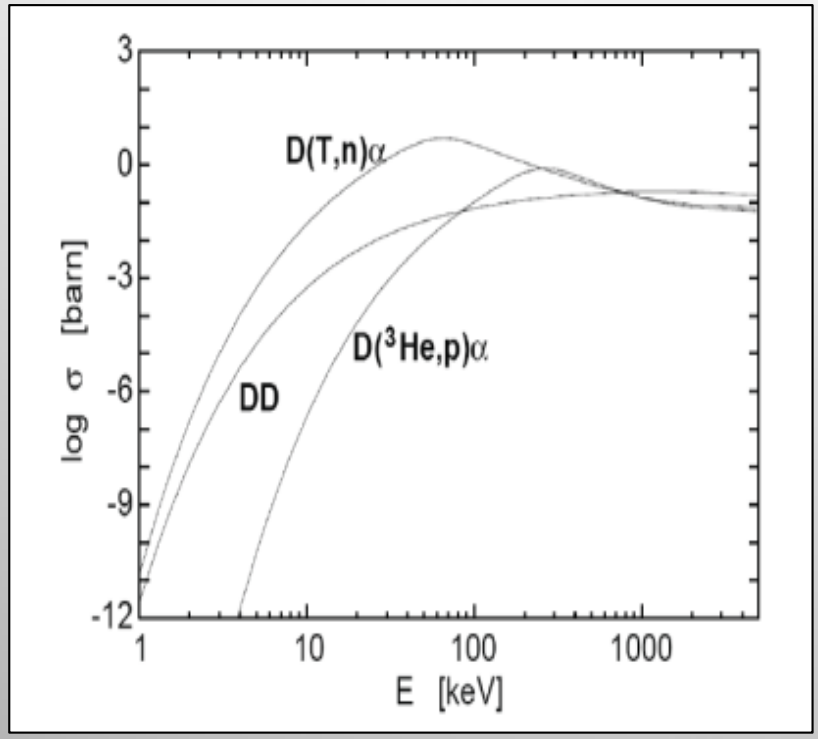

The DT reaction has the largest cross-section, ~100 times larger than any other, in the 10–100 keV energy interval

At these temperatures the atoms are ionized: plasma
The reactions involve the ions in the plasma

Fusion of light nuclei results in lower total mass
The mass difference is released as fusion energy

$\Delta E = \Delta(mc^2) = 17.6 MeV$

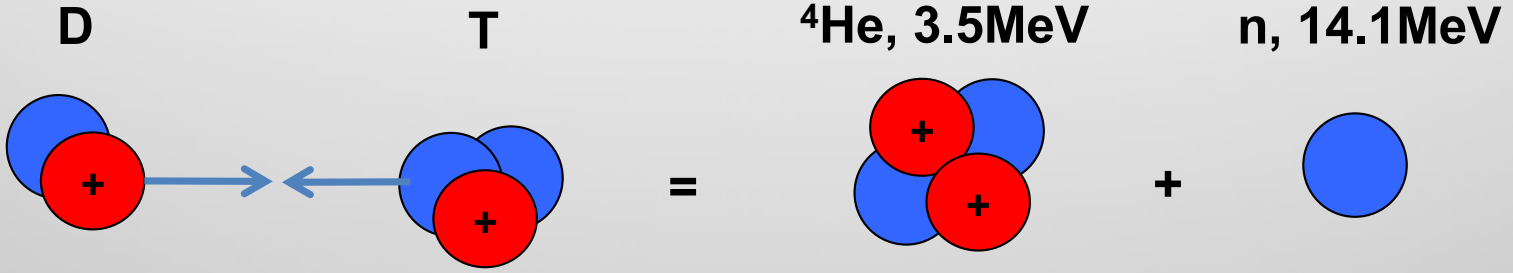

The α-particles have high cross section and release energy into the fuel (self heating).
The neutrons carry exploitable energy: n-Yield is the most important metric to assess success.

Burn rate, fractional burn, areal density

Assume equimolar, $n_D=n_T=n$, DT plasma assembled to meet fusion conditions. The burn rate is:

$$n'(t) = -(1/2) \langle\sigma v\rangle n(t)^2$$

If $\langle\sigma v\rangle$ stays constant (not true), we can integrate the equation over the confinement time τ:

$$n(\tau) = n_0 \, (n_0/2 \langle\sigma v\rangle \tau + 1)^{-1}$$

The fractional burn is: **$f=1-n(\tau)/n_0$**

$$f = n_0\tau \; / (2\langle\sigma v\rangle^{-1} + n_0\tau)$$

Plugging in $n_0=\rho/m$, we get:

$$f = (\tau\rho/m) \; / (2\langle\sigma v\rangle^{-1} + \tau\rho/m)$$

Notice: $\tau \propto$ R = radius, therefore the $\tau\rho$ terms lead to **ρR = areal density**

For areal density ~ 3g/cm^2 the fractional burn is 30% and fusion yield is ~10^5 MJ/g

Estimate confinement time, τ, for spherical DT assembly:

The mass-average radius of a uniform sphere is

$$< r >= \frac{4\pi \int r\, \rho\, r^2 dr}{4\pi \int \rho\, r^2 dr} = \frac{4\pi \int r\ r^2 dr}{4\pi \int\ r^2 dr} = \frac{3}{4} R$$

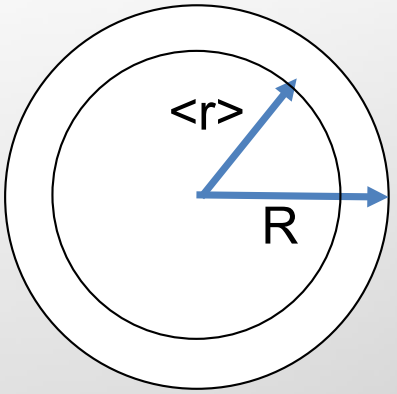

Therefore: $\tau = (R - < r >)/c_s$ c_s= sound speed ~ 3 10^{7}cm/s $\tau = R/(4c_s)$

Plugging into the equation for f we get:

$f = \rho R / (\rho R + 8mc_s/\langle\sigma v\rangle)$ $\xrightarrow[c_s \sim 3\ 10^7 cm/s]{5\text{-}30keV}$ **$f = \rho R / (\rho R + 7g/cm^2)$**

ρR= Areal density

$$f^* = f\left(\frac{3g}{cm^2}\right) = 0.3$$

Estimate fusion yield = 14.1MeV f* 1/[(3+2)amu] = 8e10 J/g

[Ref.: R. Betti - HEDP Summer School, University of California, Berkeley 12 August 2005]

It is practically impossible to ignite a whole, homogeneous, sphere of cryogenic DT fuel at $\rho R=3 g/cm^2$

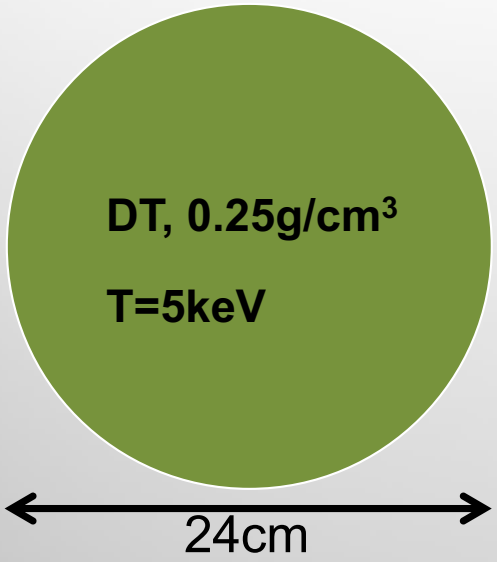

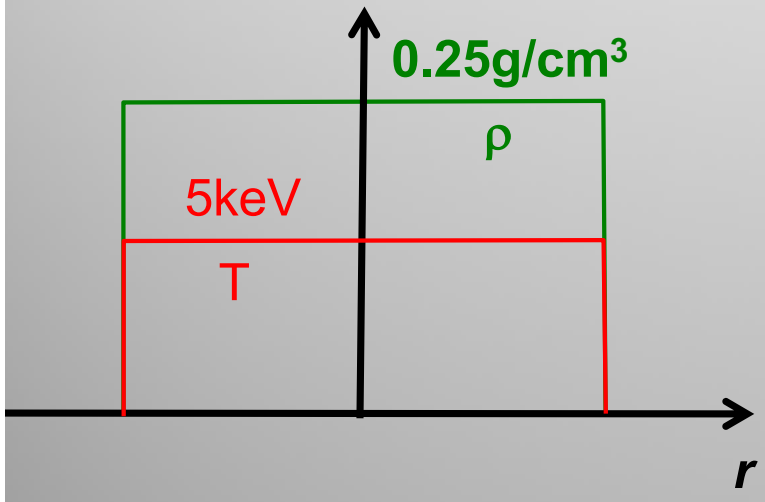

- DT solid density = $0.25 g/cm^3$
- At $\rho R=3 g/cm^2$: $R=\rho R/\rho=12cm$ and $M= 4/3\ \pi\ R^3\ \rho = 1.8kg$ of DT
- Confinement time, at 5keV: $\tau = R/(4c_s) \sim 100ns$
- 1.8kg of DT at 5keV ~ 0.35TJ. Assuming 30% energy transfer efficiency, we need ~1TJ
- Power = $1TJ/100ns = 10^7$ TW ~ 10^6 times any existing power plant
- If you managed to ignite it, it would release 150TJ ~ 35 kilotons!!!
- Change strategy: compression and hot spot ignition….

[Ref.: R. Betti - HEDP Summer School, University of California, Berkeley 12 August 2005]

Hot Spot ignition: heat only a small fraction (~1%) of compressed fuel to ignition temperatures and use self heating

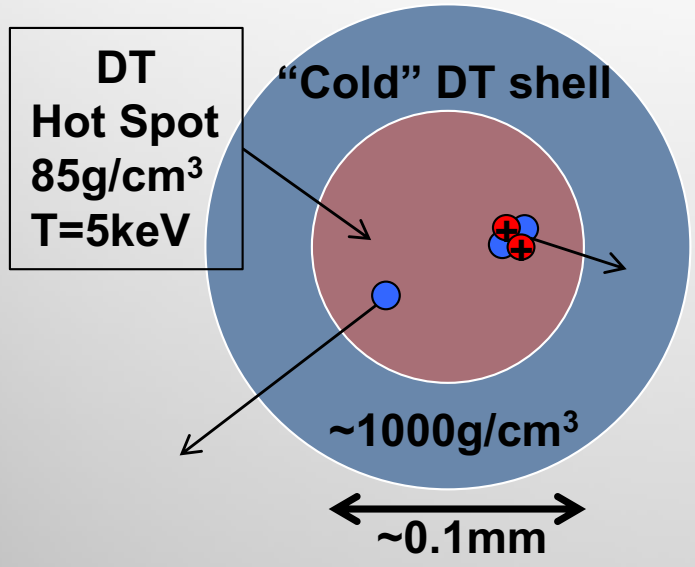

- Assume compression is achieved by laser: Typical laser pulse: t_L = 1ns
- Assume $\tau = t_L/10 = R/(4c_s)$=100ps ➔ R~0.12mm
- Assume ρR=1 g/cm^2 ➔ ρ~85g/cm^3
- Total Mass = $(4/3)\pi R^3\rho$ ~ 0.6 mg
- This mass at 5keV ~ 0.12MJ. Assuming 30% energy transfer efficiency, we need 0.39MJ.
- Power = 0.39MJ/1ns = 390TW power
- This is manageable

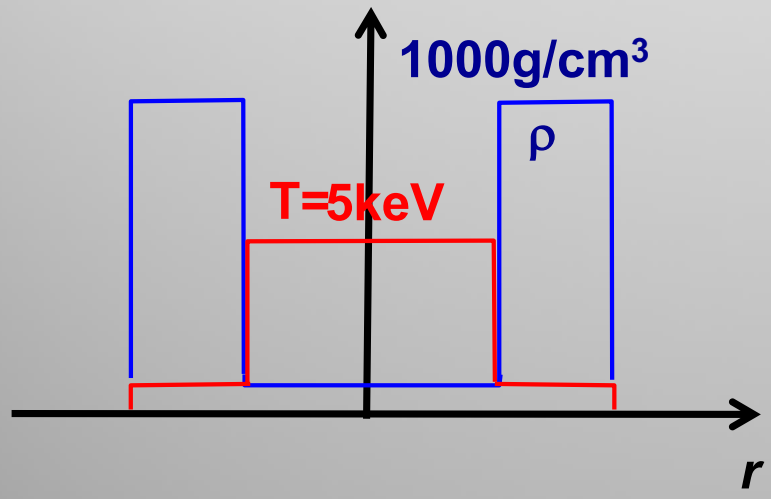

the energy released in the "hot-spot" and transported by the α-particles heats the surrounding cold fuel (self heating) to the ignition temperature: fusion burn wave.

The pressure in the H-S needs to reach $p = 0.12MJ/(4/3\ \pi\ R^3) \sim 160$ Gbar

[Ref.: R. Betti - HEDP Summer School, University of California, Berkeley 12 August 2005]

NIF can concentrate the 1.9 MJ from 192 laser beams into 1 mm^3

Matter temperature	>10 keV
Radiation temperature	>0.350 keV
Densities	>10^3 g/cm^3
Pressures	>100 Gbar

The NIF uses Indirect Drive geometry

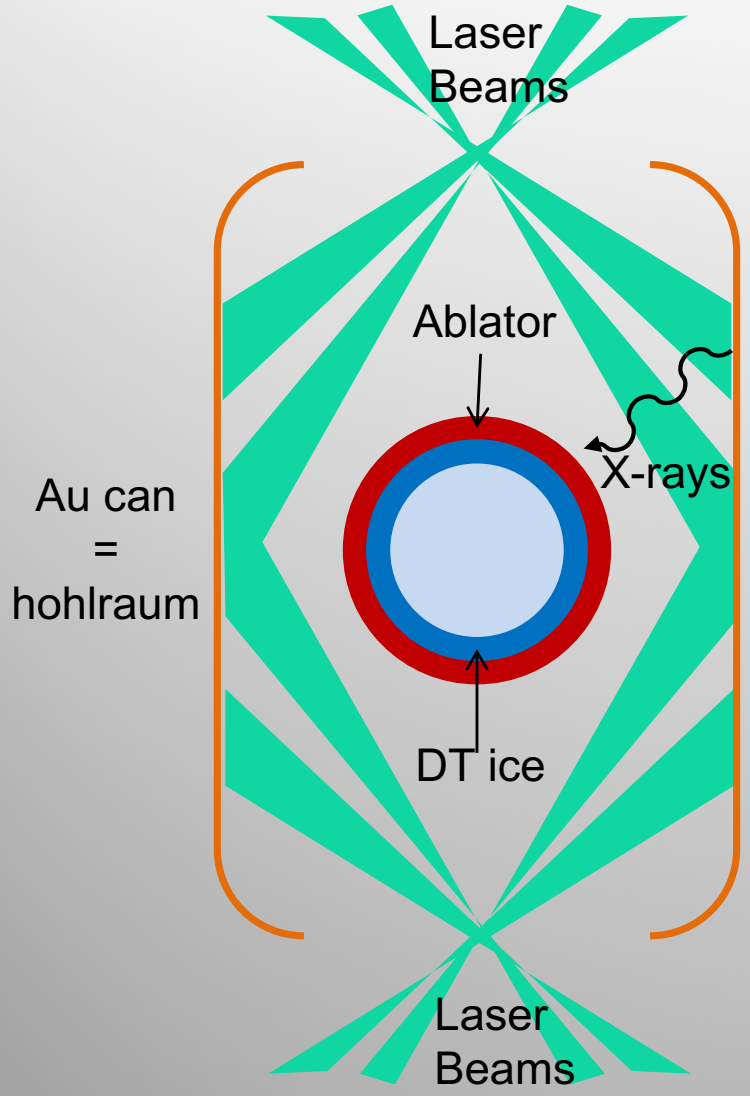

The laser beams heat the inner walls of a Au hohlraum, generating a plasma, which in turn generates X-rays

The X-ray radiation ablates the surface of the outer shell (e.g. CH) inducing an inward rocket reaction that compresses the fuel: implosion

The implosion's main purpose is to compress and act as a "pressure amplifier" and reach > 300Gbar

The hohlraum is used to improve radiation drive uniformity on the capsule=Ablator+Fuel

The trick of ICF is to turn 100 million atmospheres of pressure into 300 *billion* atmospheres of pressure

E_{laser} ~ 1.8 MJ
$E_{x\text{-}ray}$ ~ 1.3 MJ produced by hohlraum Plasma

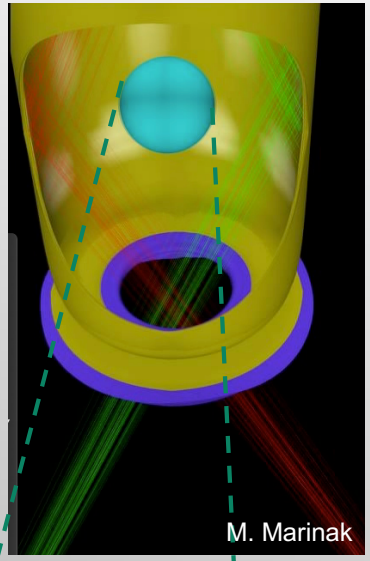

Shell Surface explodes
$E_{absorbed}$ ~ 150 kJ
$P_{ablator}$ ~ 100 Mbar

The implosion's main purpose is to compress and act as a "pressure amplifier"

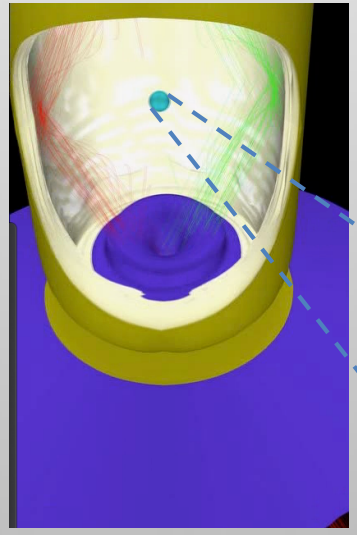

Fuel and remaining ablator accelerate inwards
KE_{fuel} ~ 14 kJ
Speed ~ 370 km/s

$P_{stagnation}$ ~ need 300+ Gbar

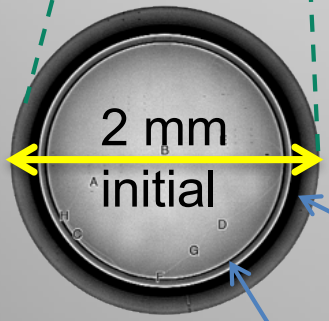

"Ablator"
(~195 microns thick)

DT ice (fuel) layer (~69 microns thick)

"hot-spot"

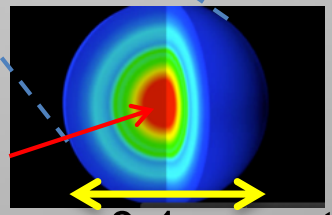

0.1 mm at stagnation

Compression in 3D is spoiled by fuel asymmetries

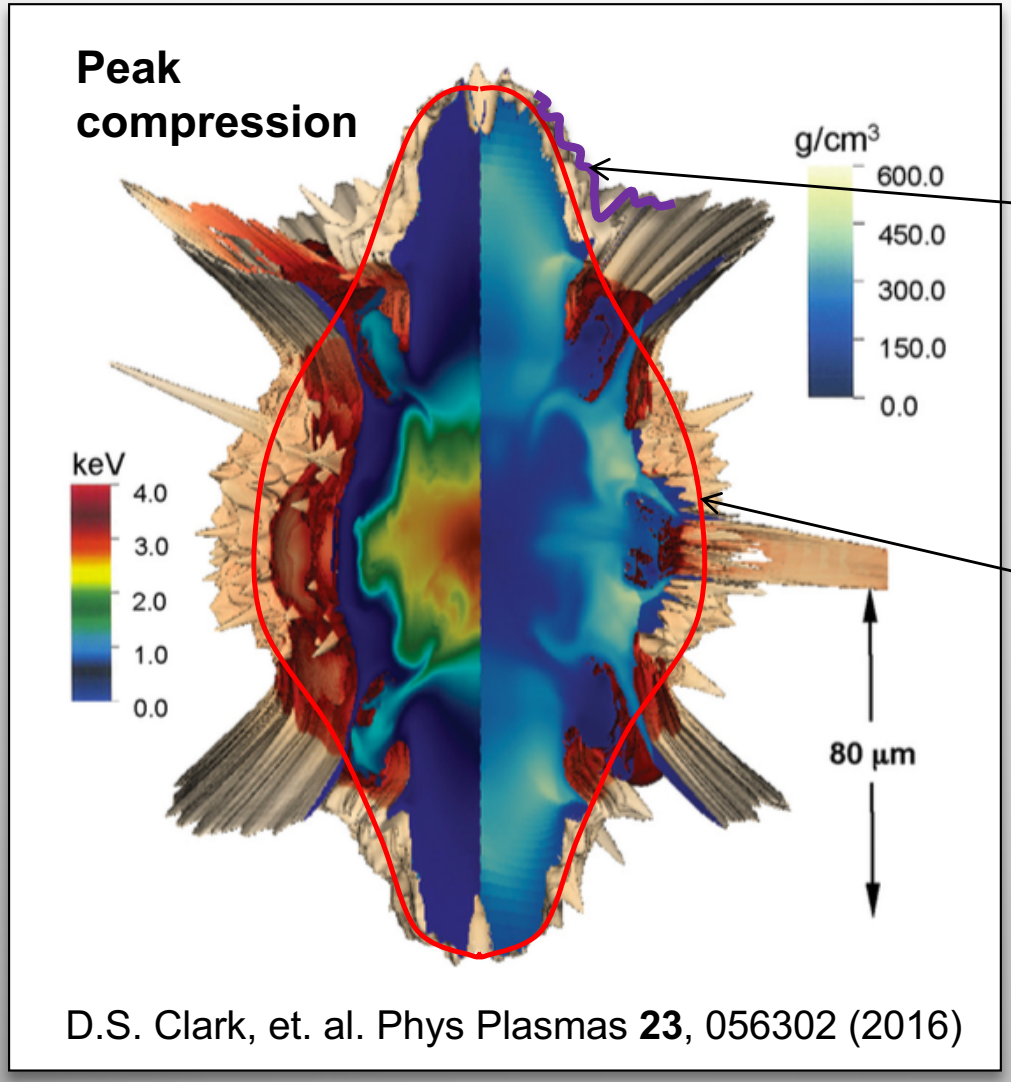

D.S. Clark, et. al. Phys Plasmas **23**, 056302 (2016)

High frequency asymmetries: seeded by target imperfections and amplified by hydro-instabilities.

Low frequency asymmetries: seeded by variations in the drive (hohlraum)

Rayleigh-Taylor instability is due to inertia

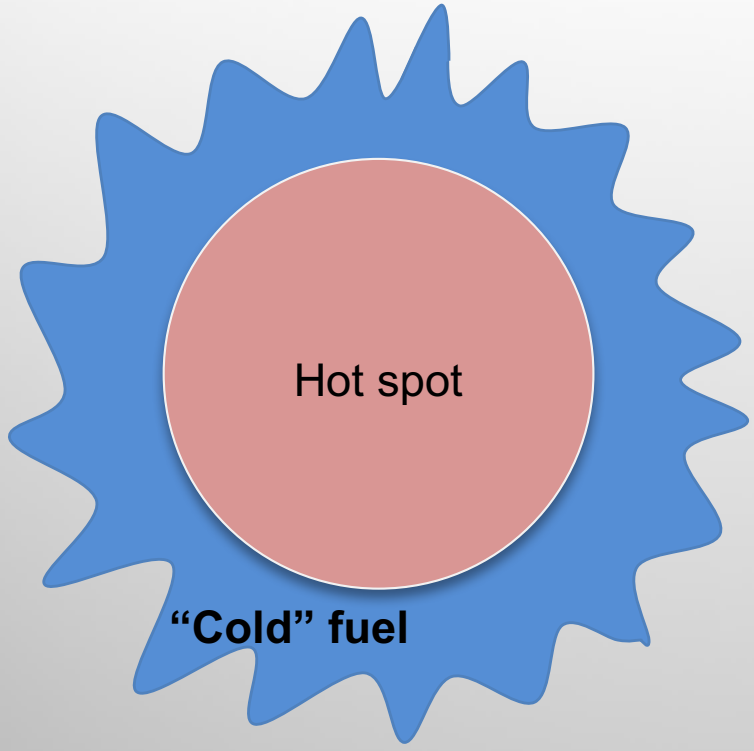

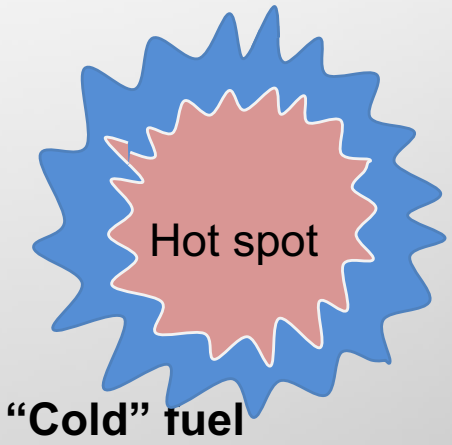

Acceleration phase: the heavy cold fuel is unstable on the outer front

Deceleration phase, the heavy cold fuel is unstable on the inner front, because heavier than hot spot

Pre-existing imperfections or defects grow in time as capsule implodes with growth rates that are amplified by instabilities.

We need to look at the imploding fuel to understand what can disrupt ignition

The imploding fuel is a plasma.

Dense plasmas are opaque to visible light. We need X-rays to image the dense plasma in the fuel: **X-ray Radiography**

Plasmas emit X-rays.
X-ray imaging using plasma X-ray sources can be used to look at the implosion.

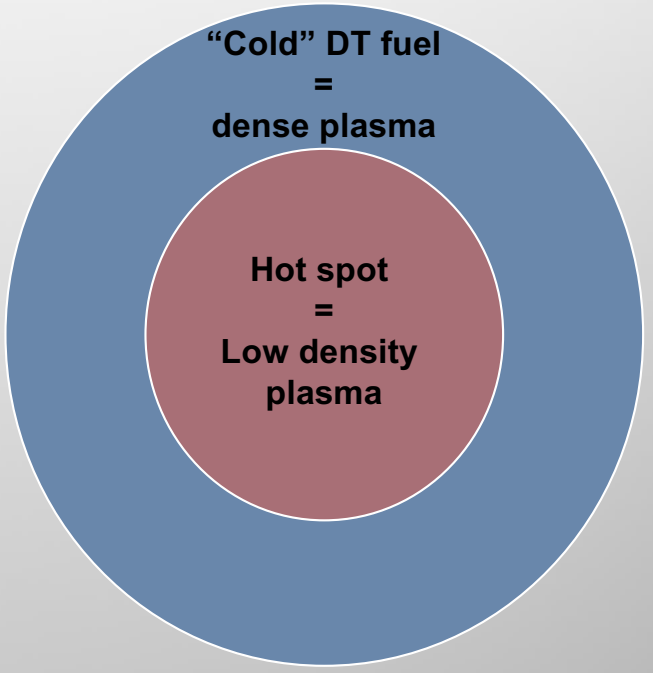

Let's look at some plasma properties →

Outlook

Motivation

- Our problem: probing ICF targets
- This requires the use of X-rays
- Plasmas are efficient sources of X-rays

Summary

- What is ICF
- Need to image ICF targets
- Laboratory-generated X-ray sources: laser plasma
  - Basic Plasma parameters
  - Basics of Radiation emission from laser-plasmas
- Imaging techniques
- Application of Radiography to ICF targets

Debye Screening

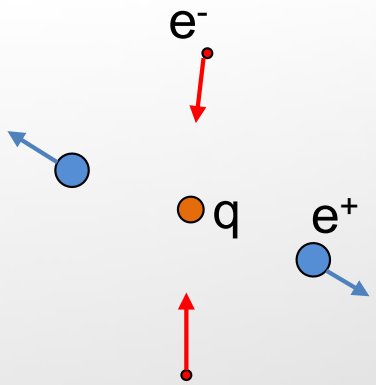

In a plasma the charges are free to move and adjust around any test charge q:

$$\nabla\phi^2 = -\frac{1}{\epsilon_0}[q\,\delta(r) + e(n_i - n_e)]$$

Assume equilibrium and Linearize Boltzmann statistics:

$$n_s = n_0 e^{e_s\phi/kT_s} \xrightarrow[e\phi \ll kT_s]{} n_0(1+e_s\phi/kT_s)$$

Need to solve:

$$\nabla\phi^2 = -\frac{1}{\epsilon_0} q\,\delta(r) + \frac{e^2 n_0}{\epsilon_0 k}\left(\frac{1}{T_i} + \frac{1}{T_e}\right)\phi$$

With $\lambda_D{}^{-2} \equiv \frac{e^2 n_0}{\epsilon_0\, k}\left(\frac{1}{T_i} + \frac{1}{T_e}\right)$

$$\nabla\phi^2 = -\frac{1}{\epsilon_0} q\,\delta(r) + \frac{\phi}{\lambda_D{}^2}$$

The solution is the Yukawa potential:

$$\phi = \frac{q}{4\pi\,\epsilon_0\, r} e^{-r/\lambda_D}$$

Debye Length

$$\phi = \frac{q}{4\pi\, \epsilon_0\, r} e^{-r/\lambda_D}$$

The Yukawa potential $\left(\sim \frac{1}{r} e^{-r/\lambda_D}\right)$ decays much faster than Coulomb potential $\left(\sim \frac{1}{r}\right)$, with decay constant ~ Debye Length: λ_D

$$\lambda_D{}^{-2} = \frac{e^2 n_0}{\epsilon_0\, k}\left(\frac{1}{T_i} + \frac{1}{T_e}\right) \rightarrow \sum_s \lambda_{D_s}{}^{-2}$$

$$\lambda_{D_s} \equiv \left(\frac{\epsilon_0\, kT_s}{e_s{}^2\, n_0}\right)^{1/2}$$

Using "laser-plasma" units

$$\lambda_{D_s}(cm) \cong \left(\frac{5.5e5\; kT(eV)}{n_0(cm^{-3})}\right)^{1/2}$$

A plasma is "quasi-neutral" when sampled with volume elements larger than the Debye sphere

Ex: T_e=5keV, n_0=1e21 cm^{-3} : λ_D=17nm

Plasma parameter and Ideality

An ideal plasma is a gas with a large number (allows us to use statistics) of charged particles (neutrals are allowed too) that are free to move. Both requests lead to the concept of plasma parameter:

1) large number inside Debye sphere: $\lambda_D{}^3 n_0 \gg 1$

2) Free to move: $$1 \ll \frac{\langle Kinetic\ Energy \rangle}{\langle Potential\ Energy \rangle} = \frac{kT}{\left(\frac{e_s{}^2}{4\,\pi \in_0 \; n_0{}^{-1/3}} \right)} = 4\pi \lambda_{D_s}{}^2 n_0{}^{2/3}$$

Leads to $1^{3/2} \ll \lambda_{D_s}{}^3 \, n_0$

Ideal Plasma: $\Lambda \equiv \lambda_D{}^3 n_0 \gg 1$ and $\frac{\langle Kinetic\ Energy \rangle}{\langle Potential\ Energy \rangle} \sim \Lambda^{2/3}$

EM field propagation in Plasmas

Apply $\mathbf{E}\sim e^{i\,\omega t}$ to a plasma. Ignore motion of heavy ions and collisions (i.e. damping).

Equation of motion for each electron: $m\,\ddot{\boldsymbol{r}} = -e\boldsymbol{E}\sim e^{i\,\omega t}$

solution: $r\sim e^{i\,\omega t}$ so that: $e\boldsymbol{E} = m\omega^2\boldsymbol{r}$ i.e. $\boldsymbol{r} = \dfrac{e}{m\omega^2}\boldsymbol{E}$

Polarization density due to displacement **r**: $\boldsymbol{P} = -ne\boldsymbol{r} = -\dfrac{ne^2}{m\omega^2}\boldsymbol{E} \equiv \epsilon_{\mathbf{0}}\chi\boldsymbol{E}$

yields: $\epsilon_{\mathbf{0}}\chi = -\dfrac{ne^2}{m\omega^2} = -\epsilon_{\mathbf{0}}\dfrac{{\omega_p}^2}{\omega^2}$

Plasma frequency: $\omega_p \equiv \left(\dfrac{ne^2}{\epsilon_{\mathbf{0}}m}\right)^{1/2}$

Refractive index un-magnetized plasma ($\mu_r \to 1$): $\eta = (\epsilon_r\mu_r)^{1/2} \xrightarrow[\mu_r\to 1]{} {\epsilon_r}^{1/2} = (1+\chi)^{\mathbf{1/2}}$

$$\eta = \left(1 - \frac{{\omega_p}^2}{\omega^2}\right)^{1/2}$$

Refractive index and critical density

$$\eta = \left(1 - \frac{{\omega_p}^2}{\omega^2}\right)^{1/2}$$

Determines the EM propagation through:

$$k = \frac{\omega}{c}\eta$$

Notice: $\frac{{\omega_p}^2}{\omega^2} = \frac{ne^2}{\epsilon_0 m\omega^2} = \frac{n}{n_c}$

Critical density: $n_c \equiv \frac{\epsilon_0 m}{e^2}\omega^2$

$$\eta = \left(1 - \frac{n}{n_c}\right)^{1/2}$$

$$n_c(cm^{-3}) \cong 1.1\times10^{21}\lambda(\mu m)^{-2}$$

- $\omega < \omega_p$ or $n > n_c$: refractive index and wave vector are pure imaginary; EM wave does not propagate and is totally reflected
- $\omega > \omega_p$ or $n < n_c$: refractive index and wave vector are are real; EM wave propagates freely

Phase and Group velocity

Rewrite:

$$1)\ k = \frac{\omega}{c}\eta(\omega)$$

$$2)\ kc = \left(\omega^2 - {\omega_p}^2\right)^{1/2}$$

Phase velocity: $v_p \equiv \omega/k$

From 1): $v_p = c/\eta = c/\left(1 - \frac{n}{n_c}\right)^{1/2}$

Group velocity: $v_g \equiv \frac{\partial\omega}{\partial k}$

From 2) : $v_g = \frac{c^2}{v_p} = \eta c = c\left(1 - \frac{n}{n_c}\right)^{1/2}$

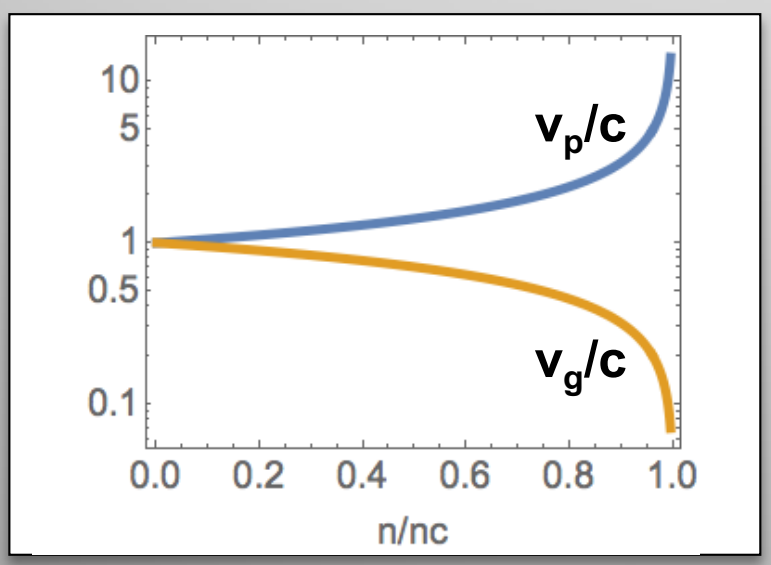

When X-rays propagate in plasma ($\omega > \omega_p$ or $n < n_c$):

$$v_p > c > v_g$$

Ponderomotive Self Focusing

Field uniform in space

$$m\,\ddot{x} = -eE(t)$$

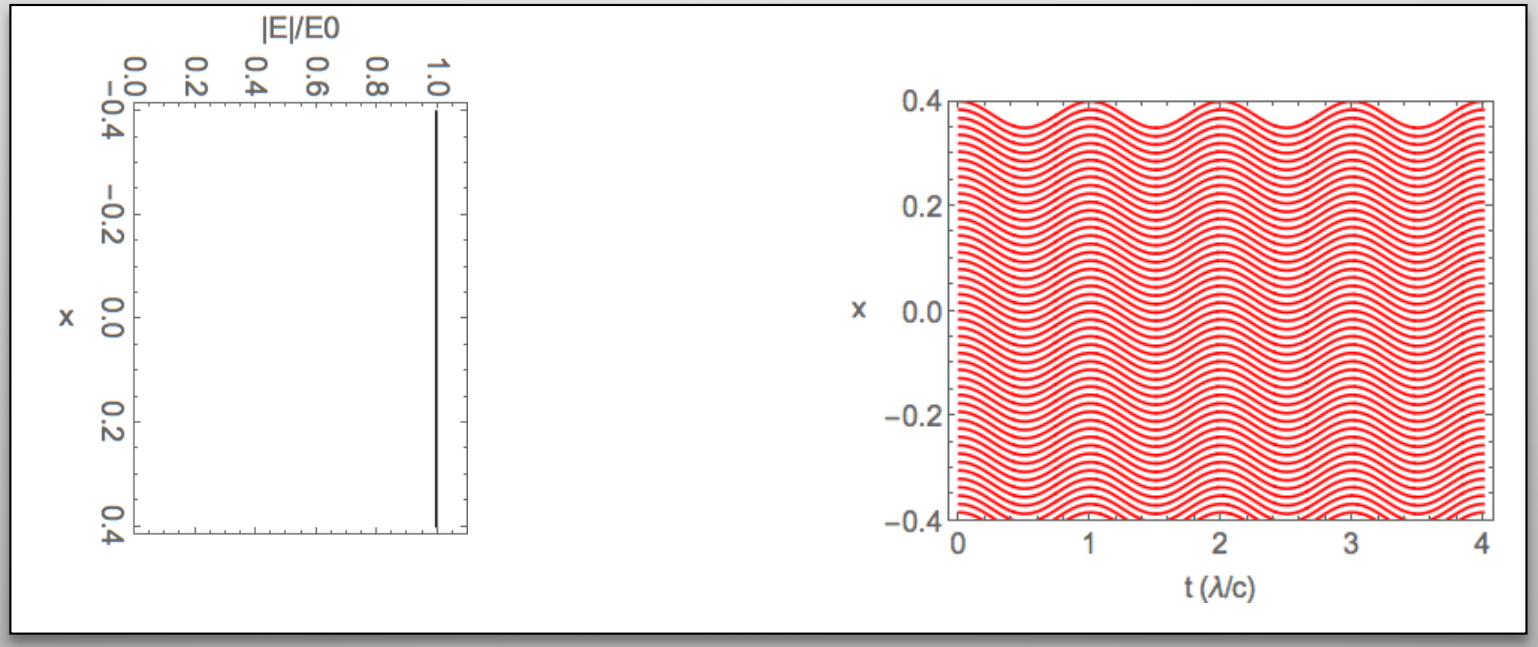

Neglect collisions: electrons oscillate with field maintaining local density

Ponderomotive Self Focusing

Field non-uniform in space (i.e. Laser beam)

$$m\,\ddot{x} = -eE(x,t)$$

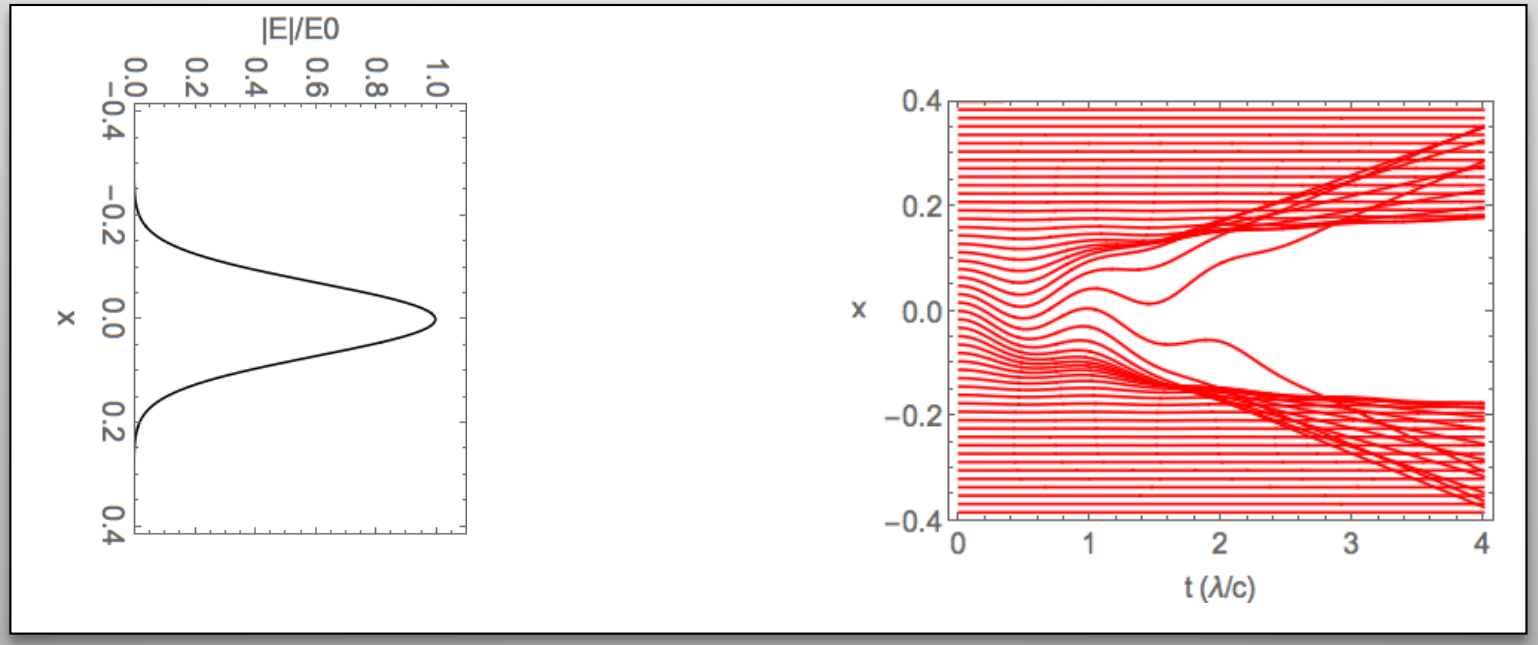

Neglect collisions: electrons are displaced from regions of strong field $F_p \propto -\nabla E^2$

Ponderomotive Self Focusing

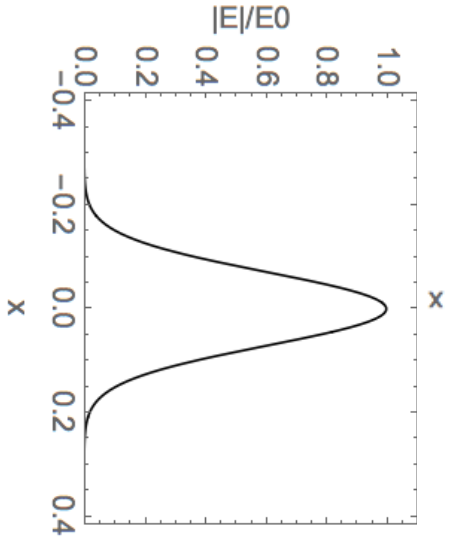

High Intensity
@ laser spot center

Electron trajectories

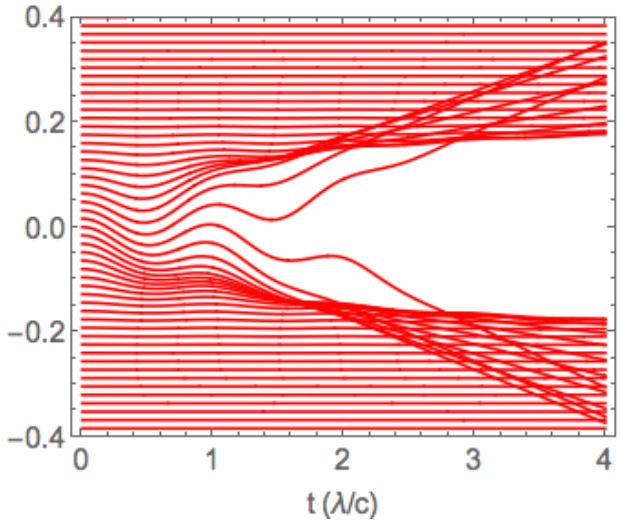

Low electron density, n,
@ laser spot center

$$\eta = \left(1 - \frac{n}{n_c}\right)^{1/2}$$

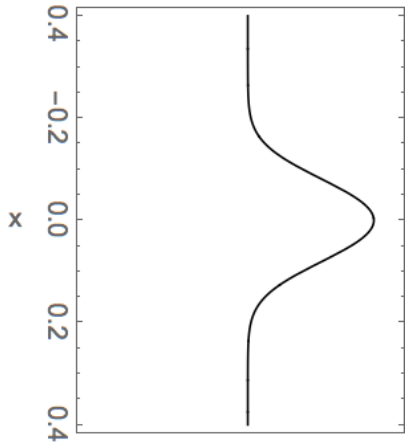

Refractive index larger
@ laser spot center

Ponderomotive force → "positive lens" refractive index → self focusing

Relativistic Self Focusing

Where EM field is very strong, electrons approach relativistic regime. We need to modify the expression for the plasma frequency:

Plasma frequency: $$\omega_p = \left(\frac{ne^2}{\epsilon_0 m}\right)^{1/2} \rightarrow \left(\frac{ne^2}{\epsilon_0 \gamma(r) m}\right)^{1/2}$$

Therefore: $$\eta = \left(1 - \frac{{\omega_p}^2}{\gamma(r)\omega^2}\right)^{1/2}$$

Also: $$n_c \equiv \gamma(r)\frac{\epsilon_0 m}{e^2}\omega^2$$

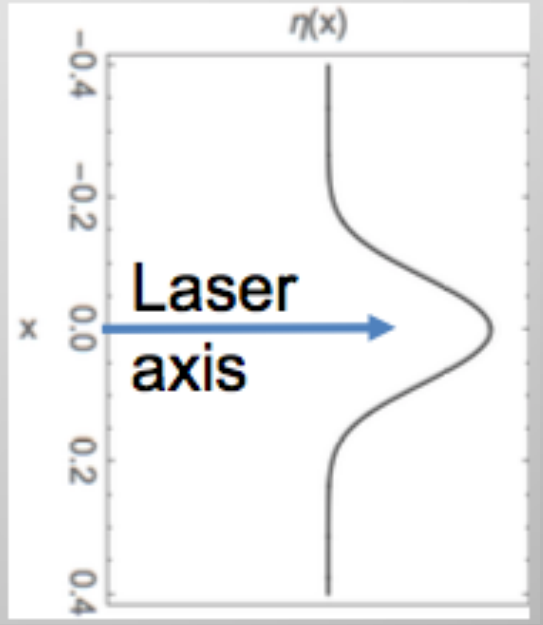

Again, we end up with a refractive index peaking on the laser axis, causing self focusing.

keV Photon energies to probe Hot Dense Matter (plasma)

$$n_c(cm^{-3}) \cong 1.1\times10^{21}\lambda(\mu m)^{-2}$$

Photon energy: $E=hc/\lambda=h\nu$

$$h\nu_c(eV) \cong 3.7\times10^{-11}\, n_c(cm^{-3})$$

Let's assume that to properly probe a plasma we need at least* $h\nu_p=10 \times h\nu_c$.

(*) This optimistic if you want to minimize refraction.

Adapted from Purvis, et. al., Nature Photon **7**, 796 (2013).

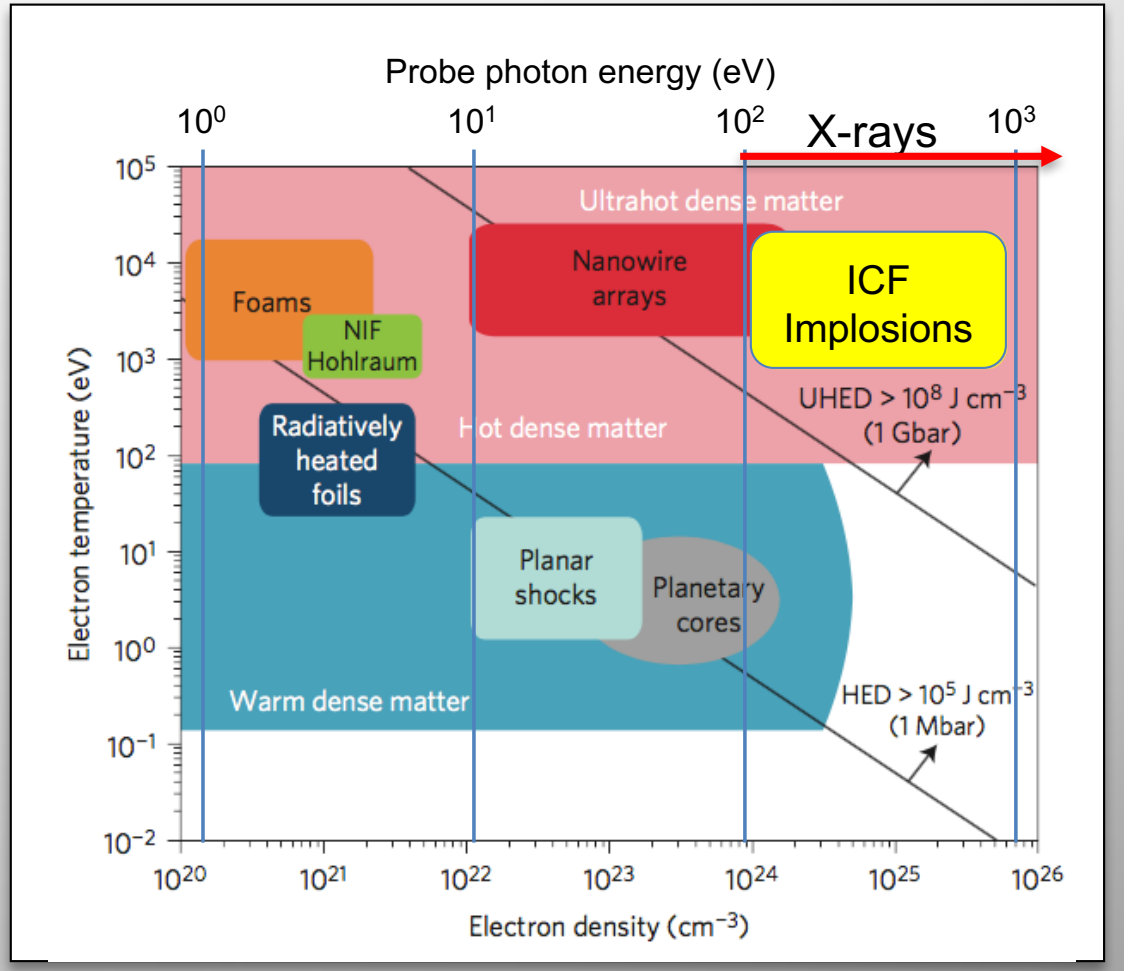

We need compact sources of X-rays: Laser generated plasmas

Outlook

Motivation

- Our problem: probing ICF targets
- This requires the use of X-rays
- Plasmas are efficient sources of X-rays

Summary

- What is ICF
- Need to image ICF targets
- Laboratory-generated X-ray sources: laser plasma
  - Basic Plasma parameters
  - Basics of Radiation emission from laser-plasmas
- Imaging techniques
- Application of Radiography to ICF targets

Laser generated plasmas

- **Main energy transfer processes: EM field ➪ Plasma**
  - **Collisional Absorption (Inverse Bremsstrahlung)**
  - **Resonance Absorption**
- **Laser Plasma interaction stages**
- **Main emission processes**
  - **Bremsstrahlung**
  - **Line emission**
  - **Recombination**

Storing EM energy into Plasma

Extracting energy back from Plasma

Collisional Absorption or Inverse Bremsstrahlung (IB)

Recall we found (in Fourier space): $\boldsymbol{r} = \frac{e}{m\omega^2}\boldsymbol{E}$

Therefore the electron oscillation (quiver) velocity is: $v_q = \frac{e}{m\omega}E_L$

Consider collisions with ions in the plasma with collision time τ_e.
The energy density contributed by the electrons to the plasma is : $\frac{n}{2}mv_q^2$

The energy density per unit time is therefore: $\frac{n}{2\tau_e}mv_q^2 = \frac{n}{2\tau_e}m\left(\frac{e}{m\omega}E_L\right)^2 = \frac{n}{n_c\tau_e}\frac{\epsilon_0 {E_L}^2}{2}$

Since $\frac{\epsilon_0 {E_L}^2}{2}$ is the Electric field energy density, the rate of absorption from the field energy is

$$\nu = \frac{n}{n_c\tau_e}$$

Using: $\frac{1}{\tau_e} = 3\,10^{-6} n\,Z\frac{ln\Lambda}{(kT)^{3/2}}$

$$\nu = 3\,10^{-6}\frac{n^2}{n_c}Z\frac{ln\Lambda}{(kT)^{3/2}}$$

higher for lower temperatures, higher Z, higher densities

Resonance Absorption (RA)

Maxwell equation: $\nabla\times\boldsymbol{B} = \epsilon\dot{\boldsymbol{E}} \xrightarrow{\text{Fourier}} \nabla\times\boldsymbol{B} = i\omega\epsilon\boldsymbol{E}$

$$0 = \nabla\cdot(\nabla\times\boldsymbol{B}) = \nabla\cdot(\epsilon\boldsymbol{E}) = \nabla\epsilon\cdot\boldsymbol{E} + \epsilon\,\nabla\cdot\boldsymbol{E} \longrightarrow \nabla\cdot\boldsymbol{E} = -\frac{\nabla\epsilon}{\epsilon}\cdot\boldsymbol{E}$$

plug in: $\epsilon = 1 - \frac{n}{n_c}$ $\qquad \nabla\cdot\boldsymbol{E} = \frac{\nabla n}{n_c - n}\cdot\boldsymbol{E}$

using $\nabla\cdot\boldsymbol{E} = -4\pi e\,\delta n$ $\qquad \boxed{\delta n = \frac{1}{4\pi e(n - n_c)}\nabla n\cdot\boldsymbol{E}}$

we are in Fourier space: δn is the amplitude of the plasma oscillation, i.e. plasma wave

If $\nabla n\cdot\boldsymbol{E} \neq 0$ A plasma wave is excited having resonant response as $n = n_c \longleftrightarrow \omega=\omega_p$

- Needs $\nabla n\cdot\boldsymbol{E} \neq 0$: it works only for oblique incidence AND p-polarization. The plasma wave can only exist longitudinal wrt the n_c surface, therefore a EM field with no component normal to the n_c surface cannot transfer energy to the plasma wave.
- At oblique incidence, ϑ, the light wave is reflected at $n(\vartheta) = n_c\cos(\theta)^2 < n_c$
- However the field can still tunnel into critical density and excite the resonance.

Resonance Absorption (RA)

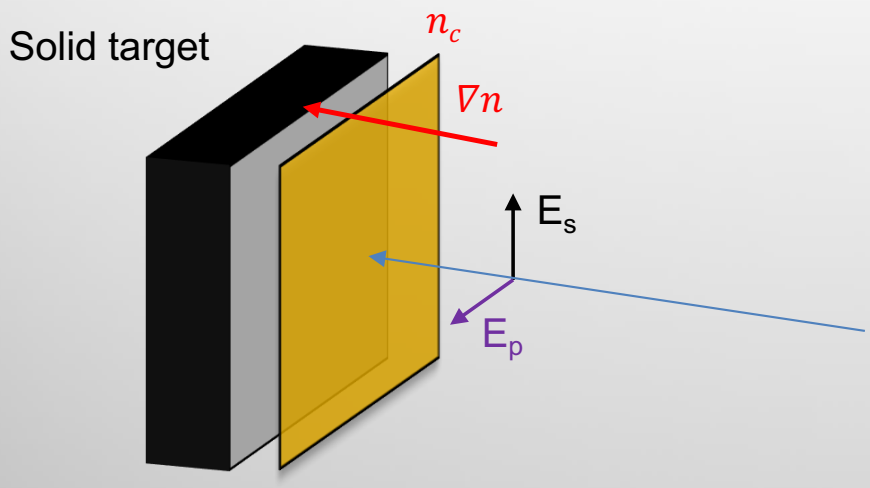

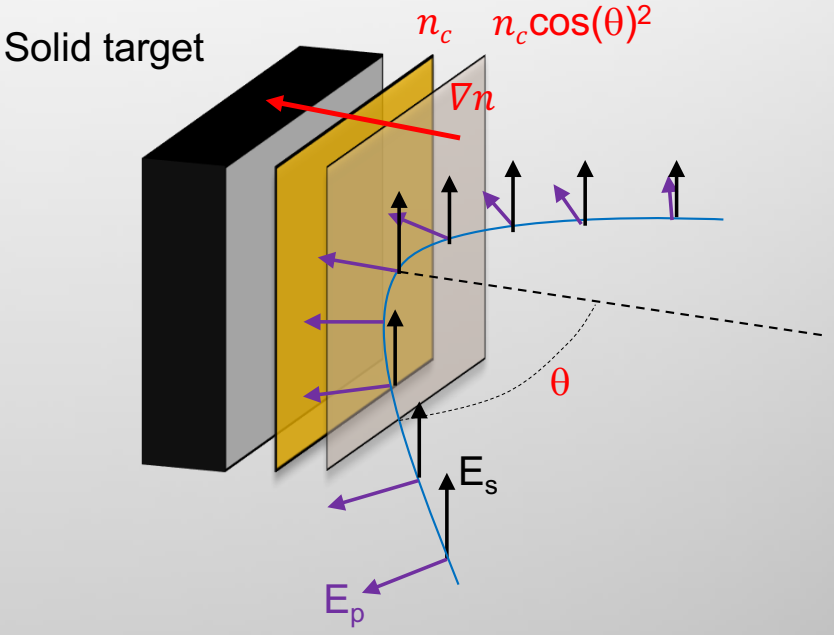

Laser incidence perpendicular to surface, i.e. parallel to ∇n.
No coupling to plasma wave possible for either E_s or E_p.

Laser incident at angle θ: E_p has a component parallel to ∇n. At the turning point E_p is totally parallel to ∇n. E_p (only) couples to plasma wave.

Laser plasma interaction stages

- low energy electrons released from solid surface by single and multi photon ionization form a low density plasma
- n_e increases: the low energy electrons absorb laser photons by IB and become energetic
- The energetic electrons collide with the target surface causing further ablation and ionization, thereby raising the electron density
- Close to target, the electron density reaches critical, $n=n_c$,: laser light cannot penetrate any further than $n_c\cos(\theta)$.
- The plasma absorbs energy mostly by RA: resonance condition achieved for the evanescent wave reaching n_c (or tunneling).
- Expansion: n drops below n_c. For laser pulses long enough the laser light interacts with underdense plasma and parametric instabilities become important: decay of photon into photon +plasma wave (Raman) or + ion acoustic wave (Brillouin).

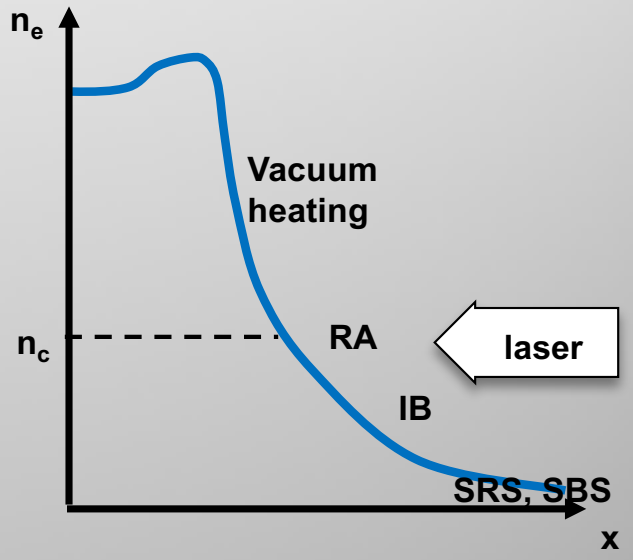

Laser-plasmas: Main emission processes

- **Bremsstrahlung:** $A + e^-(p) \rightarrow A + e^-(p') + h\nu$

  Free-Free → Continuum spectrum

- **Recombination:** $A_g^{(Z+1)+} + e^-(p) \rightarrow A_q^{Z+} + h\nu$

  Free-Bound:

  $h\nu = 1/2\ m\ v^2 + E_{Z+1}(g) - E_Z(q) = 1/2\ m\ v^2 + E_Z(\infty) - E_Z(q)$

  → **Continuum spectrum with edges (jumps) due to the condition** $h\nu \geq E_Z(\infty) - E_Z(q)$

- **Line emission:** $A_g^{Z+} \rightarrow A_q^{Z+} + h\nu$

  Bound-Bound → discrete spectrum, i.e. characteristic radiation

Bremsstrahlung functional form is easy to understand

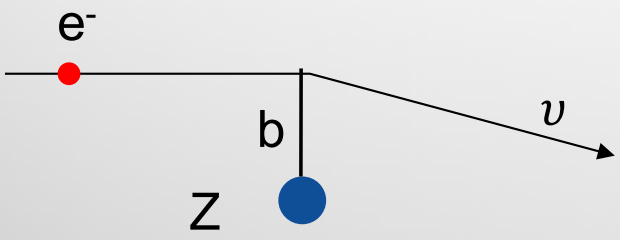

When the electron is deflected by the 'collision' with the ion, radiates due to acceleration a

$$P = \frac{2}{3}\frac{e^2 a^2}{c^3}$$

In the ion reference frame, the electron experiences a pulsed electric field of the duration of the collision. If b is the impact parameter:

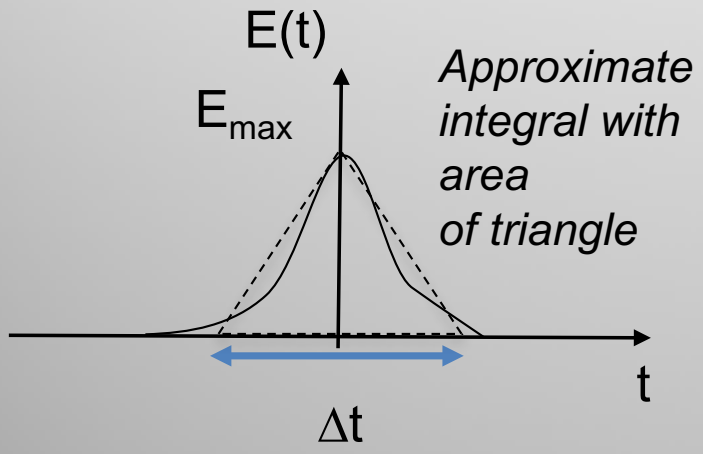

$$E_{max} = \frac{Ze}{b^2} \rightarrow \langle E \rangle = \int E dt/\Delta t \cong \frac{1}{2} E_{max}$$

$$\langle a \rangle \cong \frac{Ze^2}{2mb^2} \rightarrow P \cong \frac{1}{6}\frac{e^6 Z^2}{m^2 b^4 c^3}$$

The radiation is emitted over a time $\Delta t \propto b/v$ i.e. over a spectral width $\Delta\omega = 1/\Delta t \propto \frac{v}{b}$

Therefore, for a single electron:

$$P/\Delta\omega \cong \frac{1}{6}\frac{e^6 Z^2}{m^2 b^3 c^3 v}$$

Bremsstrahlung functional form is easy to understand

Fixed plasma parameter (Λ): $\lambda_D{}^3 \sim \Lambda / n_e$ $\quad b_{max}{}^3 = \lambda_D{}^3 \sim 1/n_e$ $\quad \langle b \rangle \sim n_i{}^{-3}$

To calculate the power emitted per unit volume and frequency, *W*, by all electrons, we multiply by the electron density n_e and integrate over a Maxwellian distribution for the electron velocities *f(v)*:

$$f(v) \propto \frac{e^{-\frac{mv^2}{2kT_e}}}{(kT_e)^{3/2}}$$

$$W_B(h\nu) \propto n_e n_i Z^2 \frac{e^{-\frac{h\nu}{kT_e}}}{(kT_e)^{1/2}} = n_e{}^2 Z \frac{e^{-\frac{h\nu}{kT_e}}}{(kT_e)^{1/2}}$$

The derivation for recombination (free-bound) is similar, however with different integration ranges due to the condition **$h\nu = 1/2\ m\ v^2 + E_Z(\infty) - E_Z(q)$**

Laser-plasmas: Summary of main emission processes

- **Bremsstrahlung:**

$$W_B(h\nu) \propto {n_e}^2 Z \frac{e^{-\frac{h\nu}{kT_e}}}{(kT_e)^{1/2}}$$

- **Recombination to level q only (sum over quantum levels):**

$$W_R(q, h\nu) \propto {n_e}^2 Z \frac{e^{-\frac{h\nu}{kT_e}}}{(kT_e)^{1/2}} \frac{Z^2}{q^3 kT_e} e^{\frac{Z^2 R_y}{q^2 kT_e}}$$

$$\frac{W_R}{W_B} \sim \frac{Z^2}{kT_e}$$

Bremsstrahlung dominates over Recombination at high temperatures or low Z

- **Line emission:**

$$W(h\nu) \propto n_Z(p) A(p,q) h\nu_{p,q}$$

$A(p,q)$ = spontaneous emission coefficient

Emission from the solid part of the target

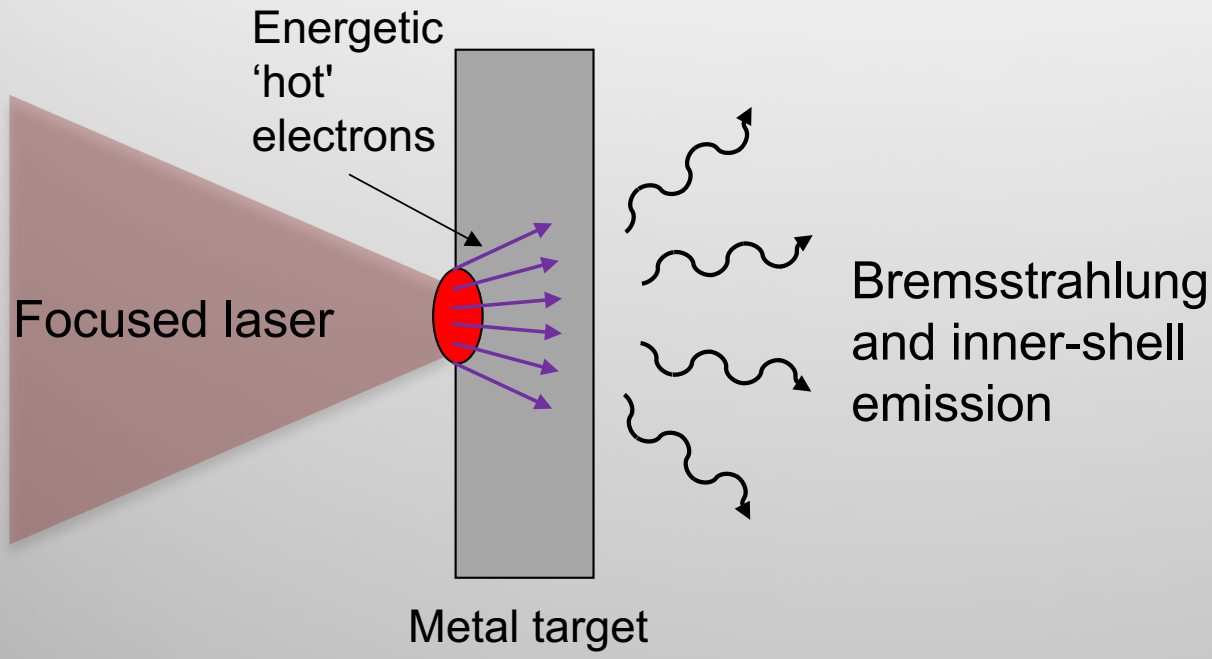

Bremsstrahlung

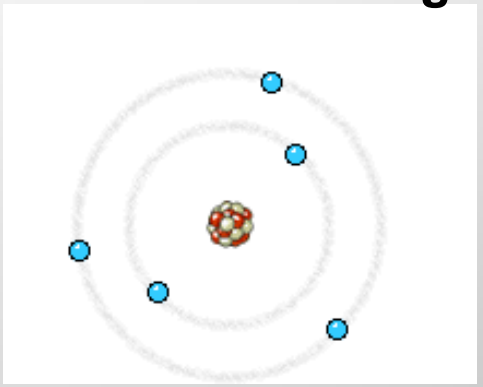

K–shell radiation

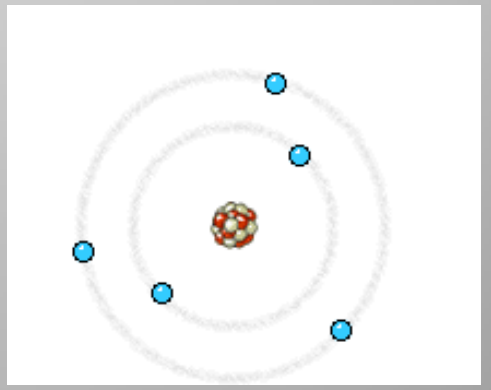

Collective absorption mechanisms transfer part of the energy to hot electrons, which are accelerated to multi-keV (i.e. to relativistic velocities) and penetrate the solid thus producing x-rays by K-shell ionization + bremsstrahlung.

Hot electron temperature scaling

Recall electron quiver velocity: $$v_q = \frac{e}{m\omega} E_L \rightarrow \frac{v_q}{c} \cong \mathbf{0.84}\left(\frac{\boldsymbol{I}}{\mathbf{10^{18}}\boldsymbol{W/cm^2}} \frac{\boldsymbol{\lambda^2}}{\mu\boldsymbol{m^2}}\right)^{\mathbf{1/2}}$$

i.e. More efficient at longer wavelengths.

The hot electron energy spectrum depends on the absorption mechanisms of field-imparted oscillations on the plasma:

$$kT \propto \begin{cases} \left(\boldsymbol{I\lambda^2}\right)^{\frac{1}{3}} \rightarrow Beg\ scaling\colon\ consistent\ with\ resonance\ absorption \\ \left(\boldsymbol{I\lambda^2}\right)^{\frac{1}{2}} \rightarrow Wilks\ scaling\colon\ consistent\ with\ ponderomotive\ acc. \end{cases}$$

Outlook

Motivation

- Our problem: probing ICF targets
- This requires the use of X-rays
- Plasmas are efficient sources of X-rays

Summary

- What is ICF
- Need to image ICF targets
- Laboratory-generated X-ray sources: laser plasma
  - Basic Plasma parameters
  - Basics of Radiation emission from laser-plasmas
- Imaging techniques
- Development of fast X-ray backlighters for ICF
- Application of Radiography to ICF targets

Area Backlighting

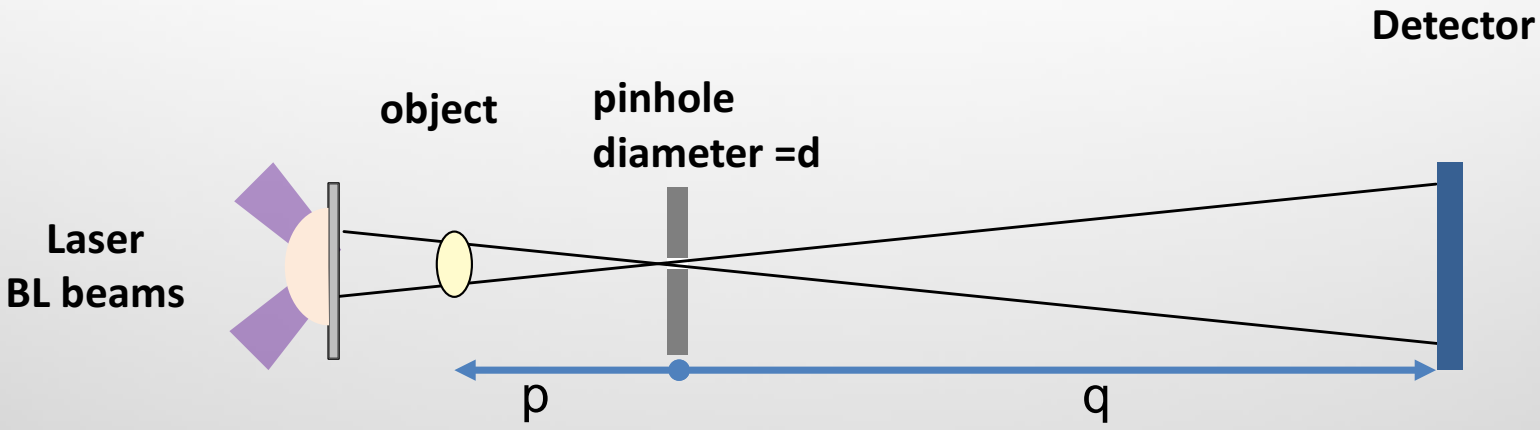

Needs Backlighter larger than object

Magnification: $M = q/p$

Resolution at object plane: $\sigma^2 = \sigma_{geom}^2 + \sigma_{diff}^2$

$$\sigma_{geom} = \frac{\frac{d}{p}(q+p)}{M} = d\left(\frac{1}{M}+1\right) \qquad \sigma_{diff} = 2.44\frac{\lambda\frac{q}{d}}{M} = 2.44\lambda\frac{p}{d}$$

Optimal pinhole diameter: $\frac{\partial\sigma}{\partial d} = 0 \rightarrow d_{opt} = \left(\frac{2.44\,p\lambda}{1+1/M}\right)^{1/2}$ $\sigma_{opt} = \sqrt{2}\left(\frac{2.44\,p\lambda}{d_{opt}}\right) = \sqrt{2}d_{opt}\left(\frac{1}{M}+1\right)$

In practice $p/d \approx 10^4$, and for 1keV BL energy $\sigma_{diff} \lesssim 3\mu m$. Therefore $\sigma \cong \sigma_{geom} \xrightarrow[M\gg1]{} d$.

Note: this applies to the case of self emission imaging as well.

Pinhole Imaging example

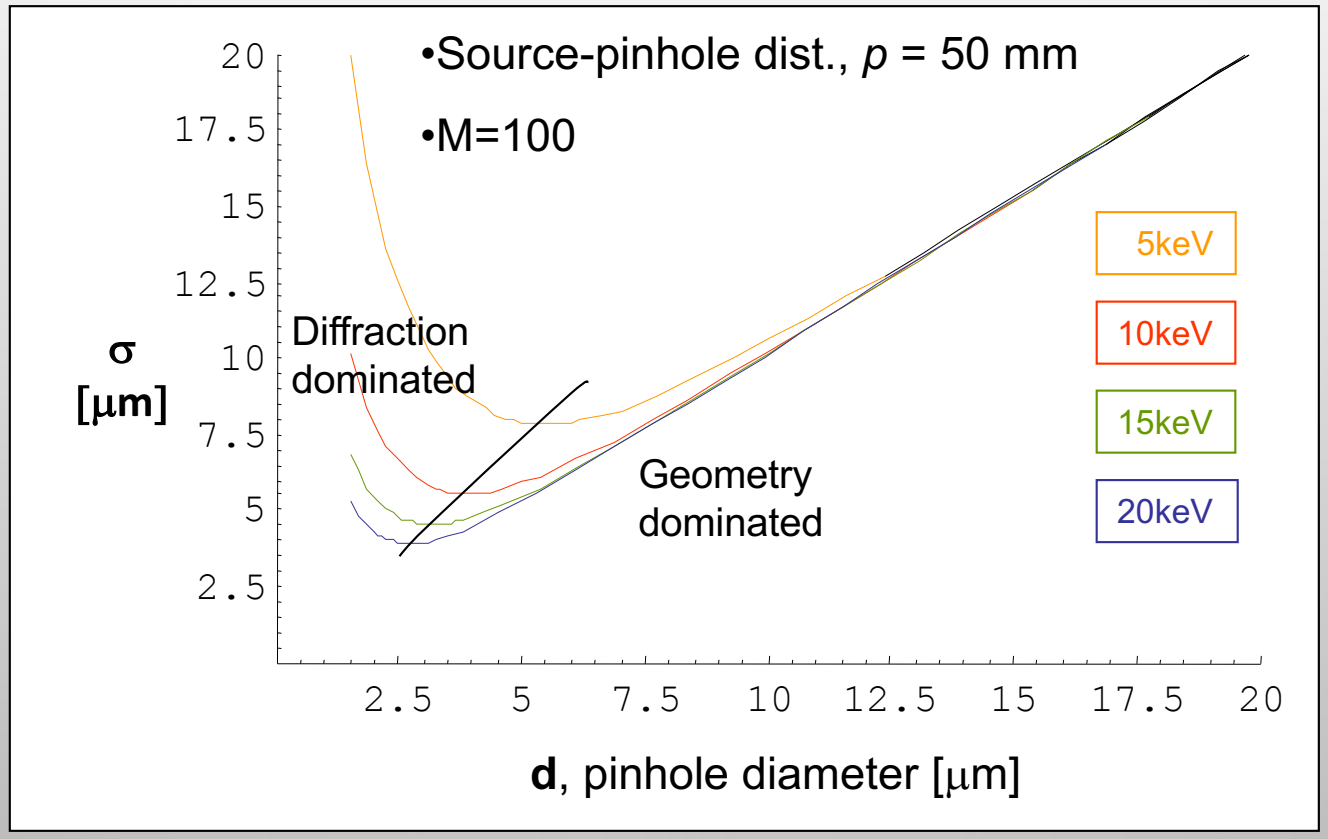

2D gated radiography: measure evolution of imploding capsule shape, ρR non uniformity and mass remaining

R. Rygg, et. al., Phys. Rev. Lett. 112 195001 (2014)

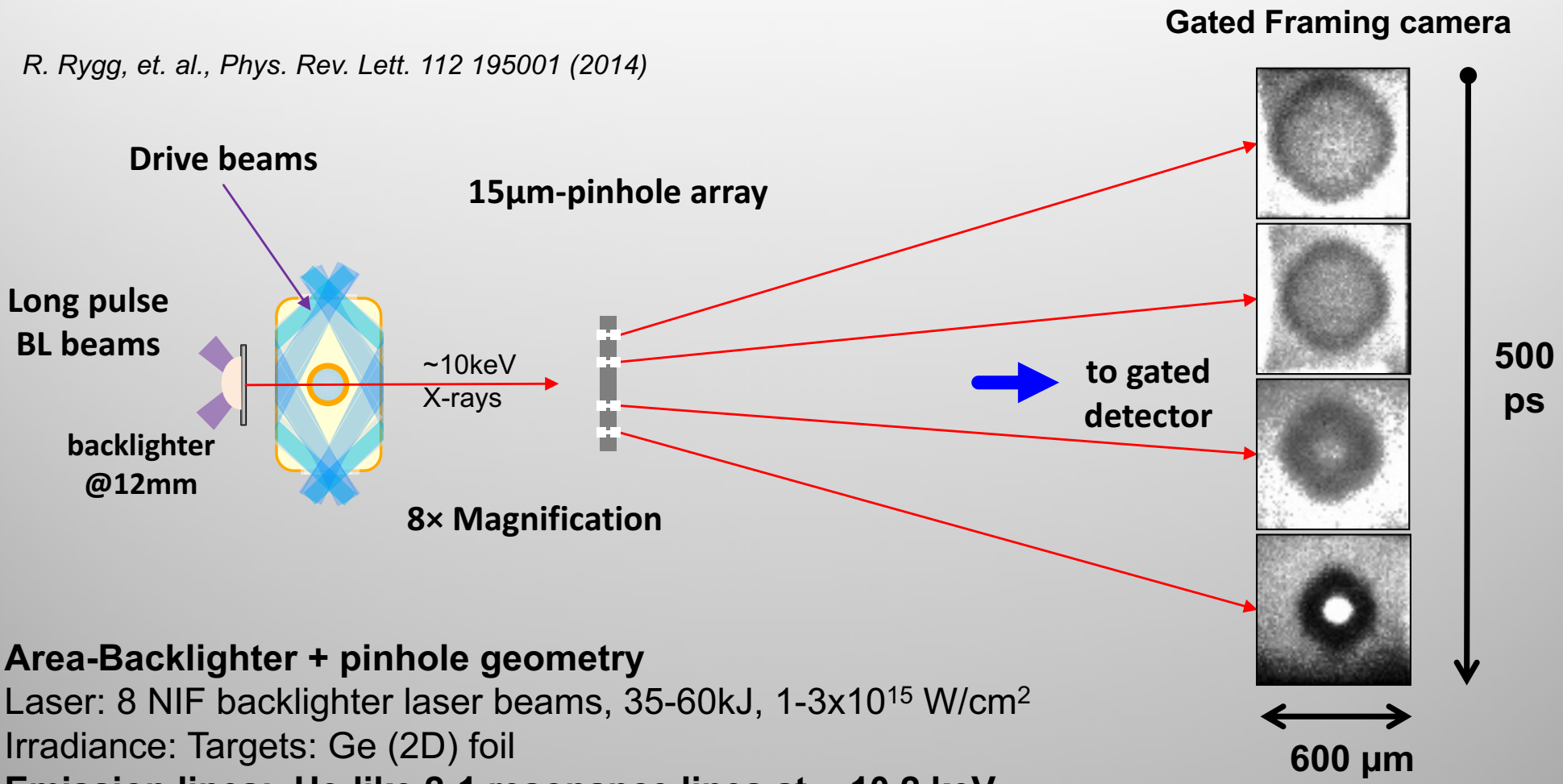

Area-Backlighter + pinhole geometry
Laser: 8 NIF backlighter laser beams, 35-60kJ, 1-3x10^{15} W/cm^2
Irradiance: Targets: Ge (2D) foil
Emission lines: He-like 2-1 resonance lines at ~ 10.2 keV
X-ray efficiency: ~1%
15*µ*m and 90 ps resolution over 400*µ*m field of view

Streaked 1D radiography: measure in-flight ablator shell profiles, velocity, mass remaining

Hicks, D. G. et al., Phys Plasmas 19, 122702 (2012)

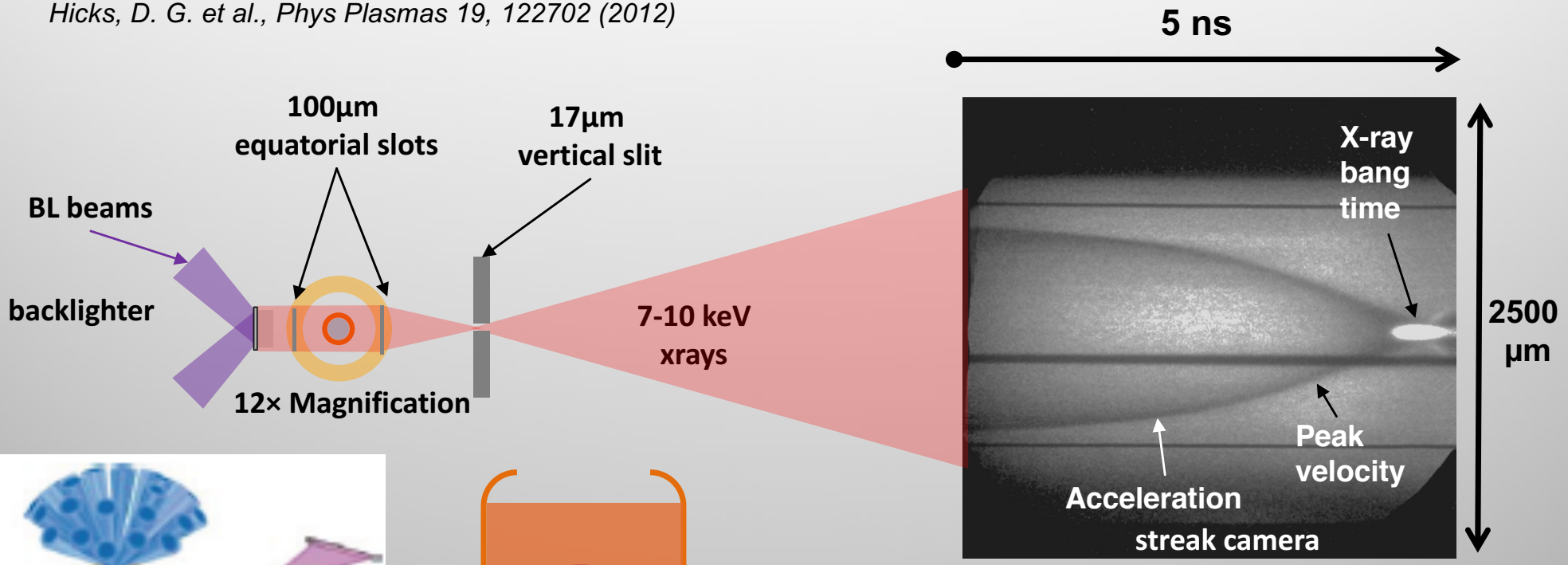

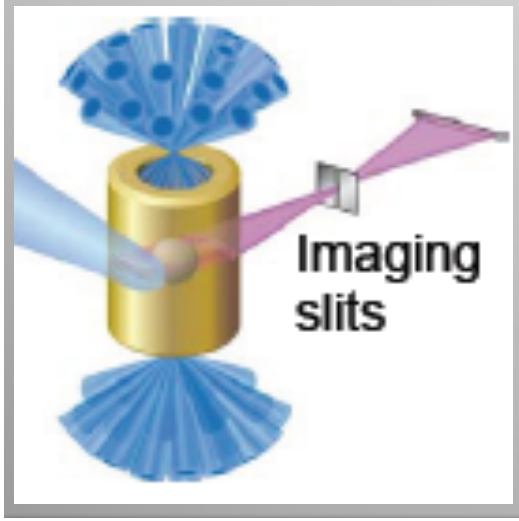

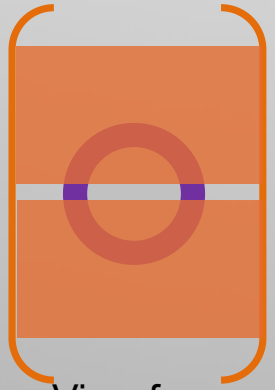

17μm, 30 ps resolution over R = 500 to 150 μm

Issues with these setups

Issues related to area backlighting experiments:

Backlighter structure is superimposed to object radiograph

Need large size Backlighter: low intensity

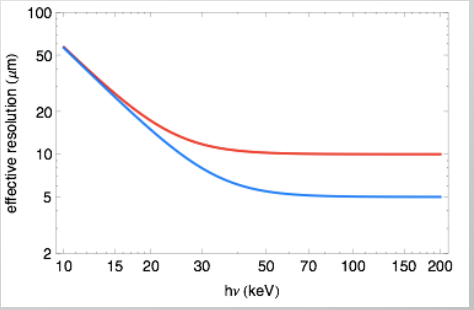

Issues related to low-energy X-rays

Refraction due to electron density gradients

Difficult to beat the core self emission (peak @~5-15 keV)

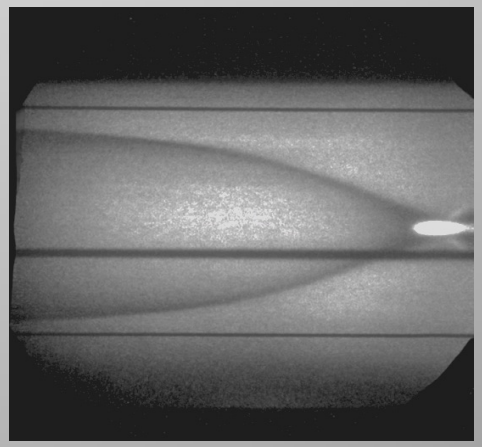

Point projection Backlighting

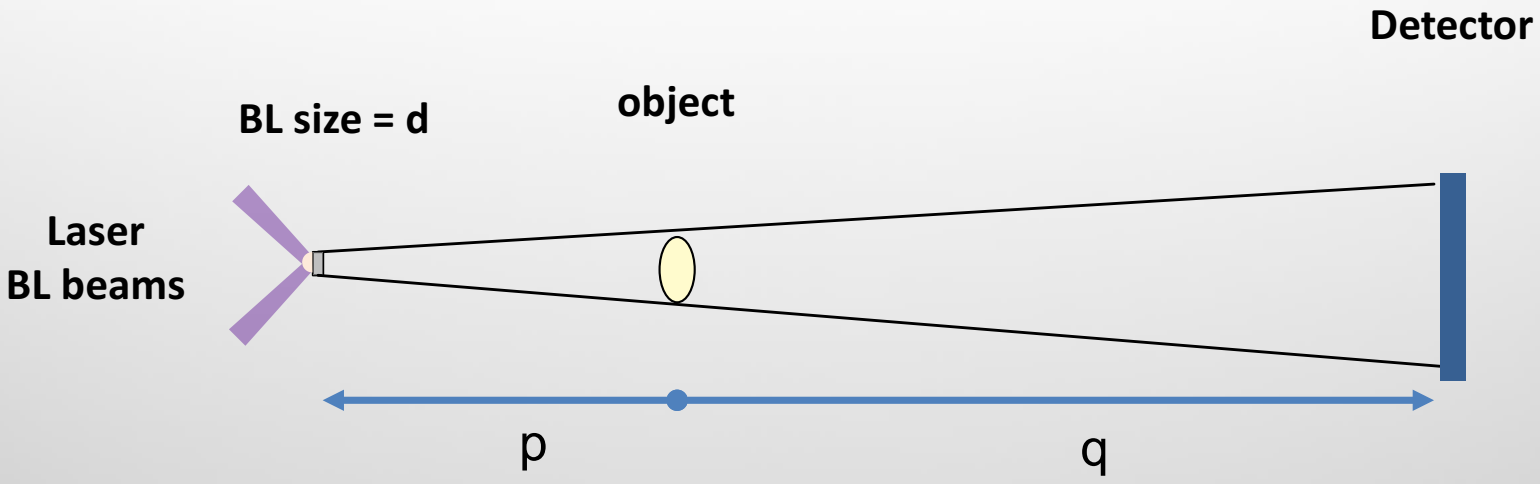

Magnification: $M = 1 + q/p$

Resolution at object plane: $\sigma = d\left(1 - \frac{1}{M}\right) \underset{M \gg 1}{\longrightarrow} d$

Advantages wrt Area Backlighting:

- Use tight focus, i.e. High laser intensities
- No pinholes
- No BL structure superimposed to object radiograph

Outlook

Motivation

- Our problem: probing ICF targets
- This requires the use of X-rays
- Plasmas are efficient sources of X-rays

Summary

- What is ICF
- Need to image ICF targets
- Laboratory-generated X-ray sources: laser plasma
  - Basic Plasma parameters
  - Basics of Radiation emission from laser-plasmas
- Imaging techniques
- Development of fast X-ray backlighters for ICF
- Application of Radiography to ICF targets

Main photon-induced processes

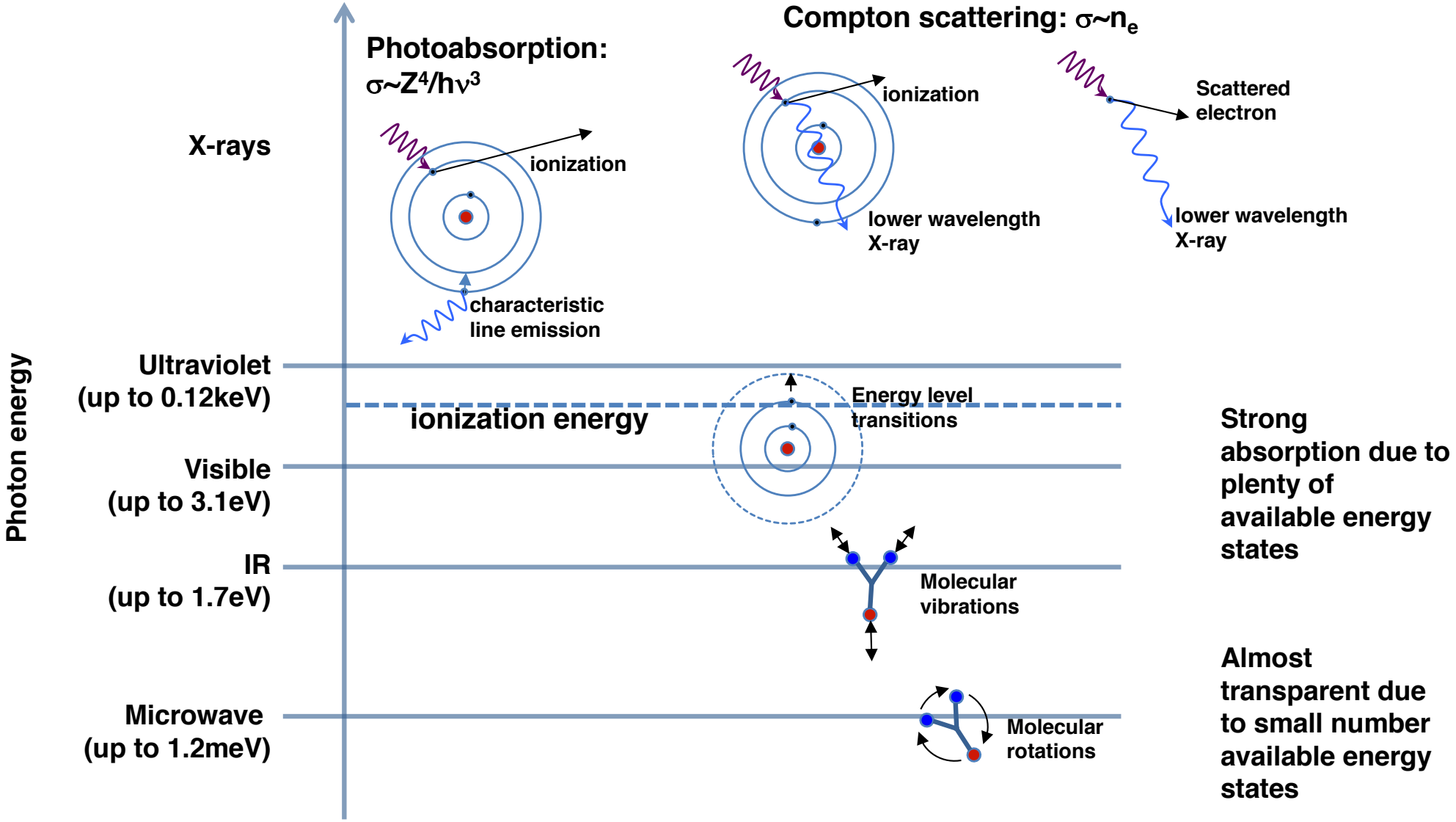

Compton Radiography (>40keV) measures the fuel areal density and asymmetries near stagnation

PoP 18, 2011

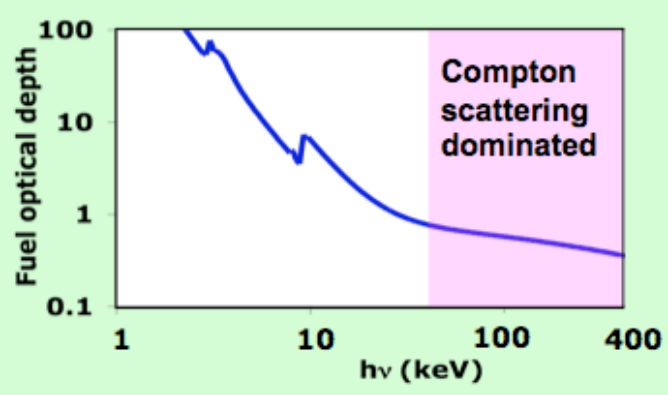

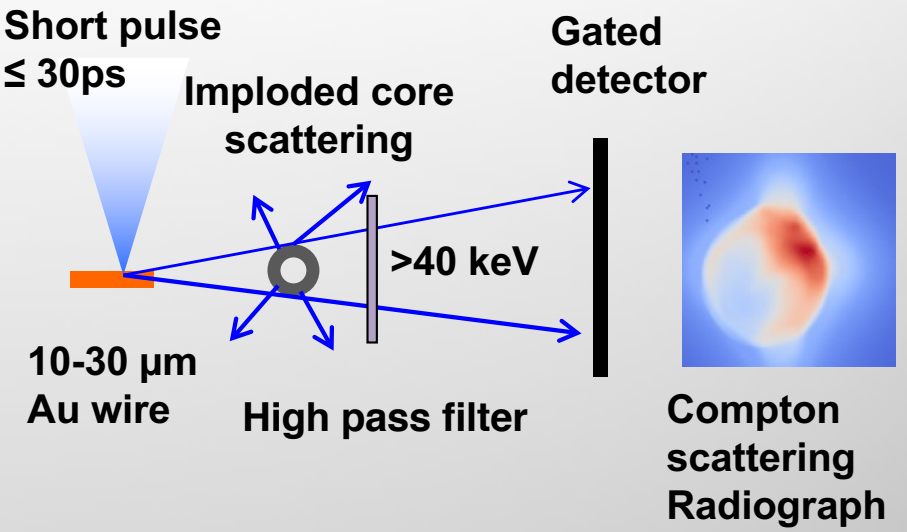

- Flat cross section: broadband, Bremsstrahlung sources are good
- Sensitive to high n_e, not high Z, therefore ideal for probing DT
- ★ Use of high x-ray photon energy minimizes refraction blurring due to strong n_e gradients. Remember: $\eta = \left(1 - \frac{n}{n_c}\right)^{1/2}$
- ★ Backlighter signal is easily separated from self emission (peak @~5-15 keV): will allow radiography at peak compression
- Point-projection geometry

Compton Radiography: demonstrated at OMEGA + (10ps, 10μm) resolution backlighters

> 60 keV radiographs achieved SNR ~ 200 over 10 μm resolution element

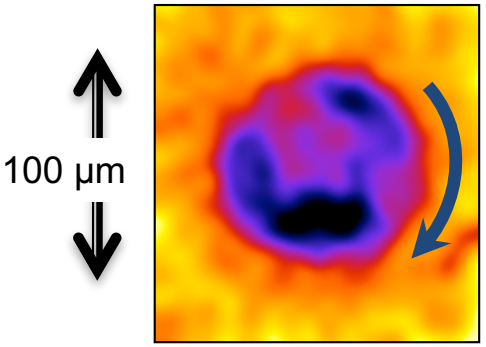

Color Key:
Orange-to-black only -10%

Mass density profile from Abel inversion

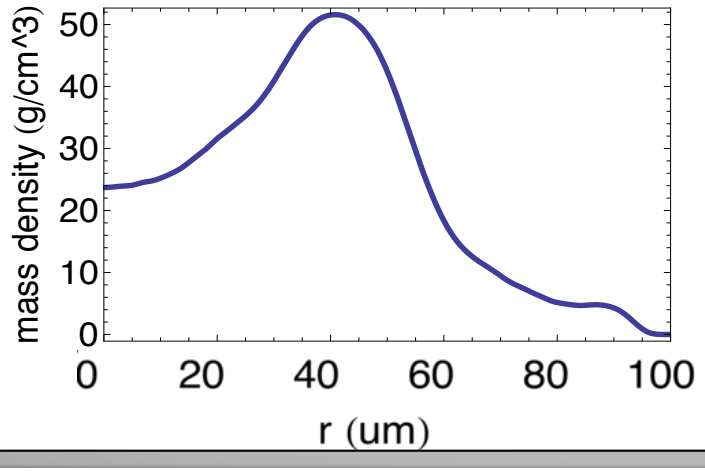

Average ρR vs time

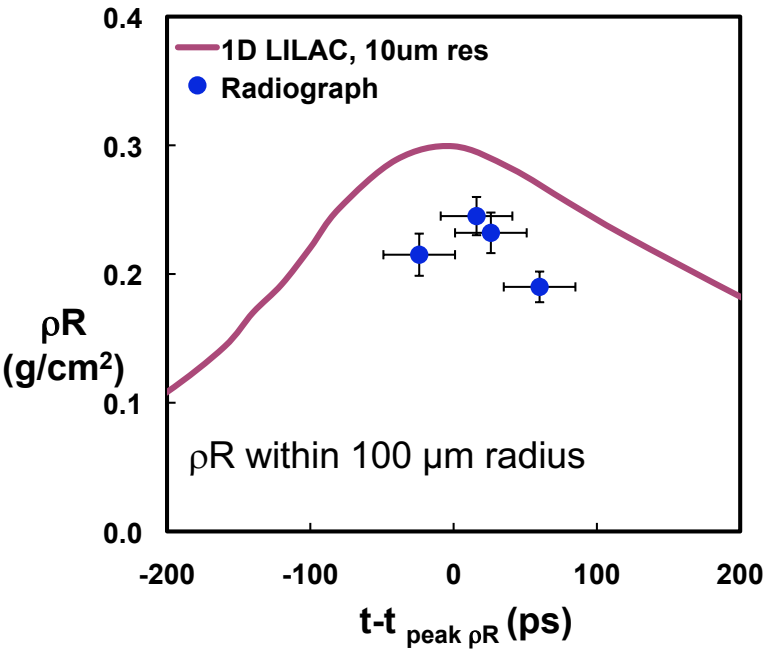

PoP 18, 2011

High intensity 1ω is required for higher conversion efficiency to hot electrons and Bremsstrahlung

Hot electron kT and C.E. ~ $(I\lambda^2)^{1/3}$

Bremsstrahlung Brightness ~ $E_L(I\lambda^2)^{1/3}=I\tau(I\lambda^2)^{1/3}$

PoP, 2017

Characterization of fast Bremsstrahlung backlighters to be used for Compton Radiography on the NIF

R Tommasini,et al.,PoP, 2017

Signal levels through different Cu thicknesses allow reconstruction of spectrum

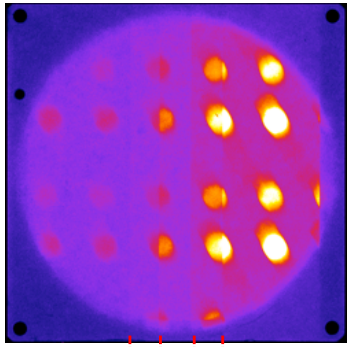

Radiograph of known calibrated object allows reconstruction of backlighter spatial profile

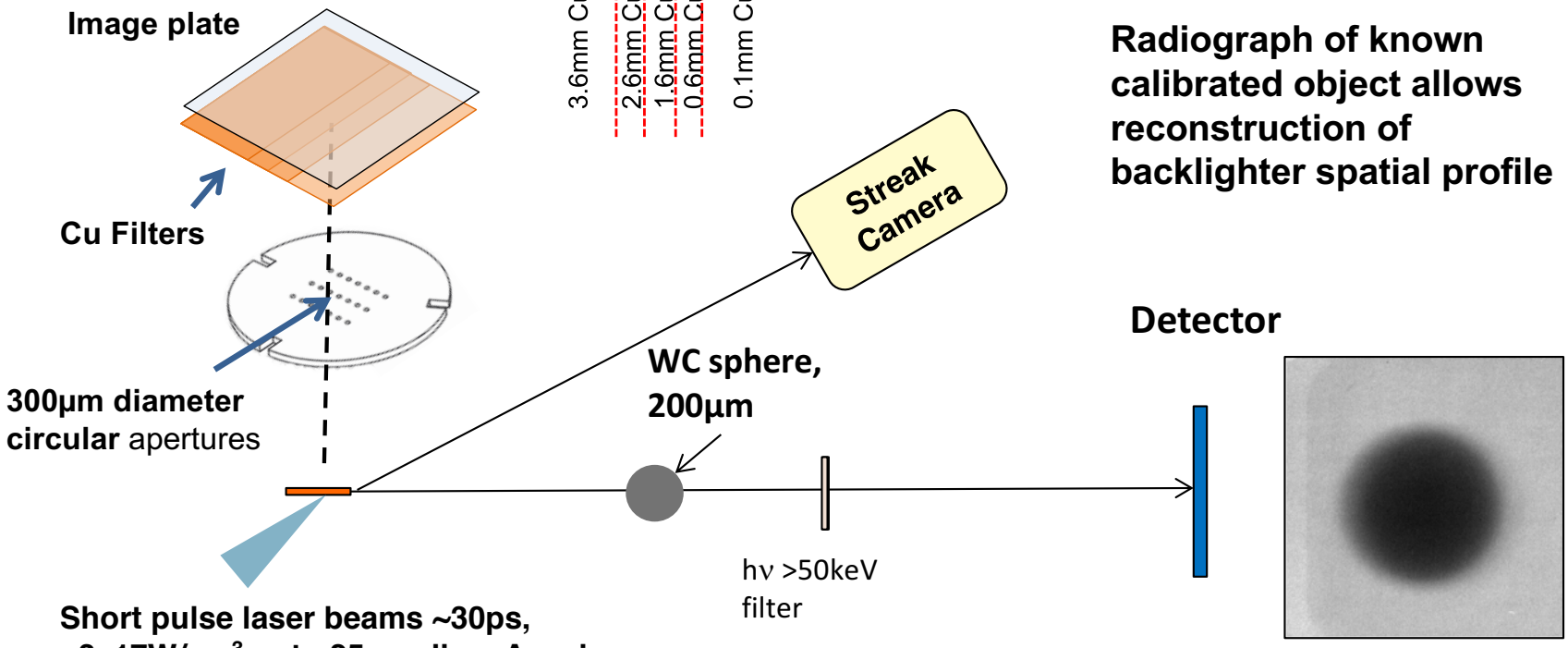

Reconstruction of the continuum bremsstrahlung emission produced by 25-μm diameter Au wires

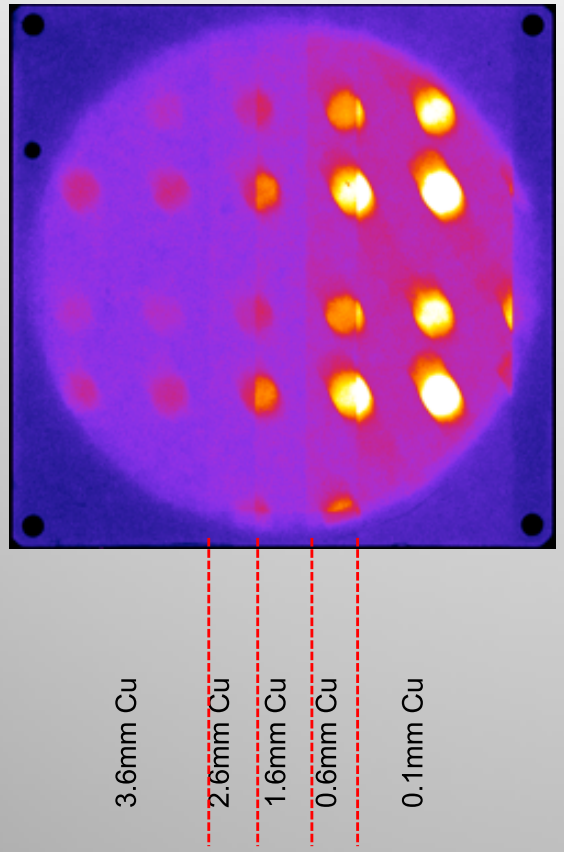

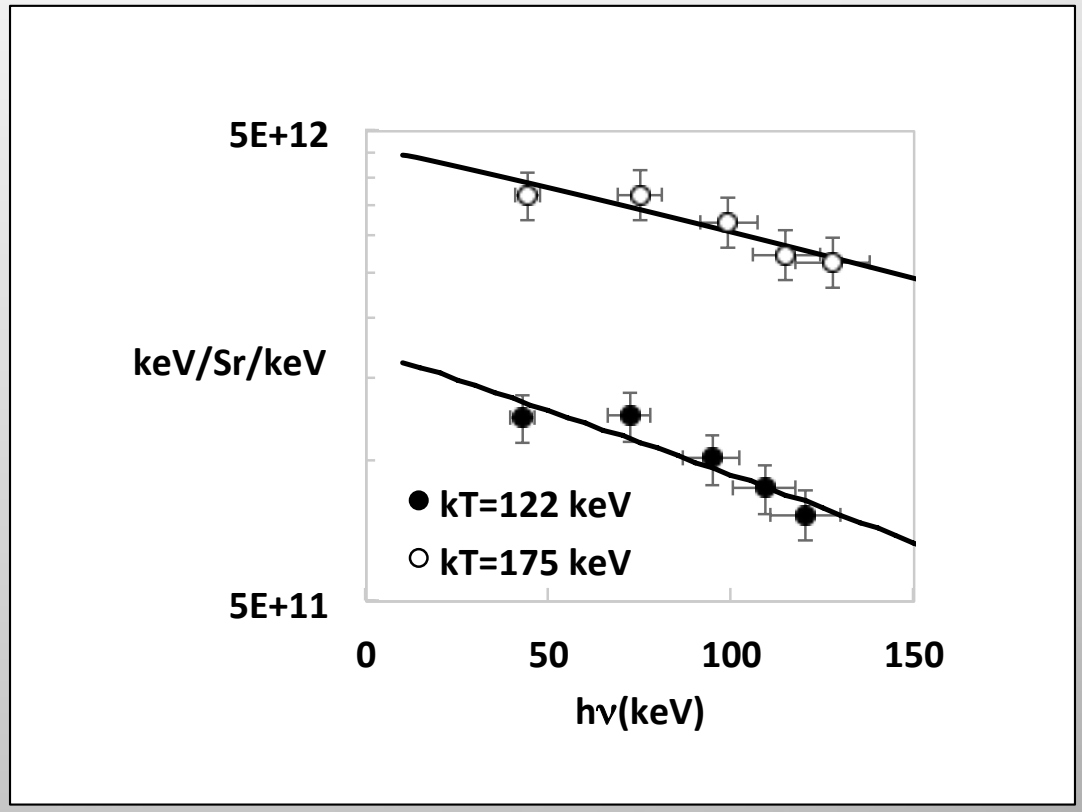

R Tommasini,et al.,PoP, 2017

Best CE(J/J) ~ 8E-4

X-ray yield into 70–200 keV energy band, vs. hot electron temperature:

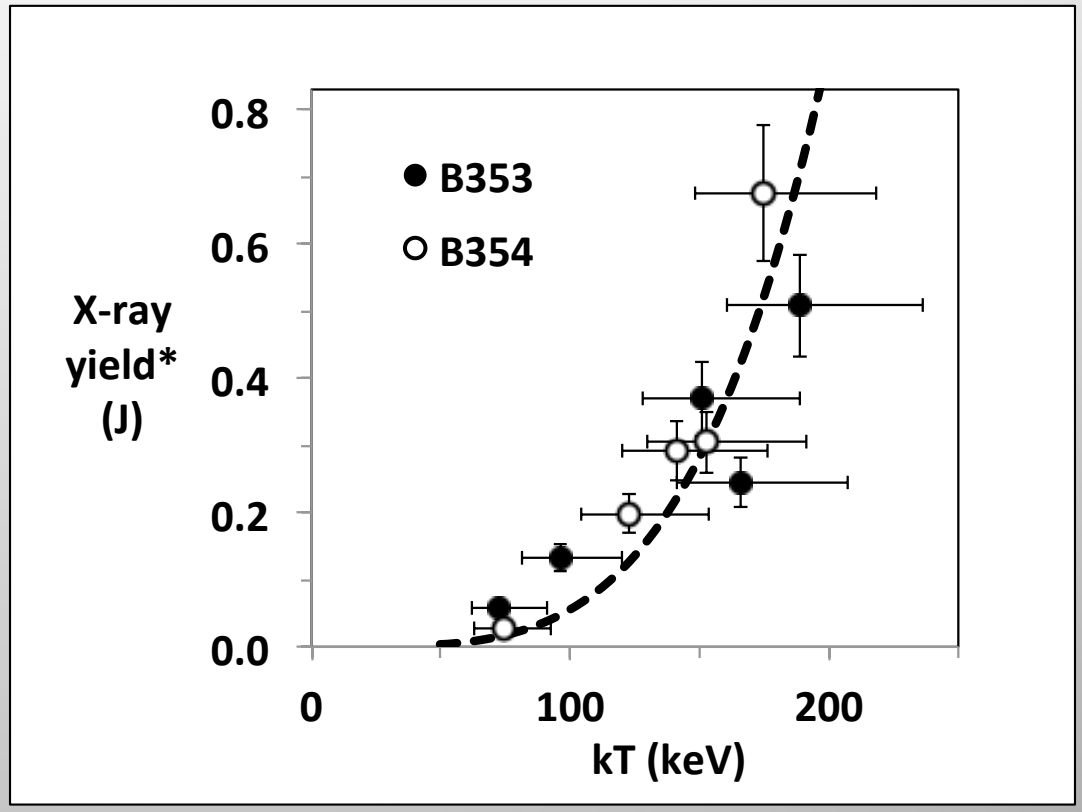

R Tommasini,et al.,PoP, 2017

FWHM duration for the backlighter emission = (32+/-3) ps i.e. ~ Laser pulse duration

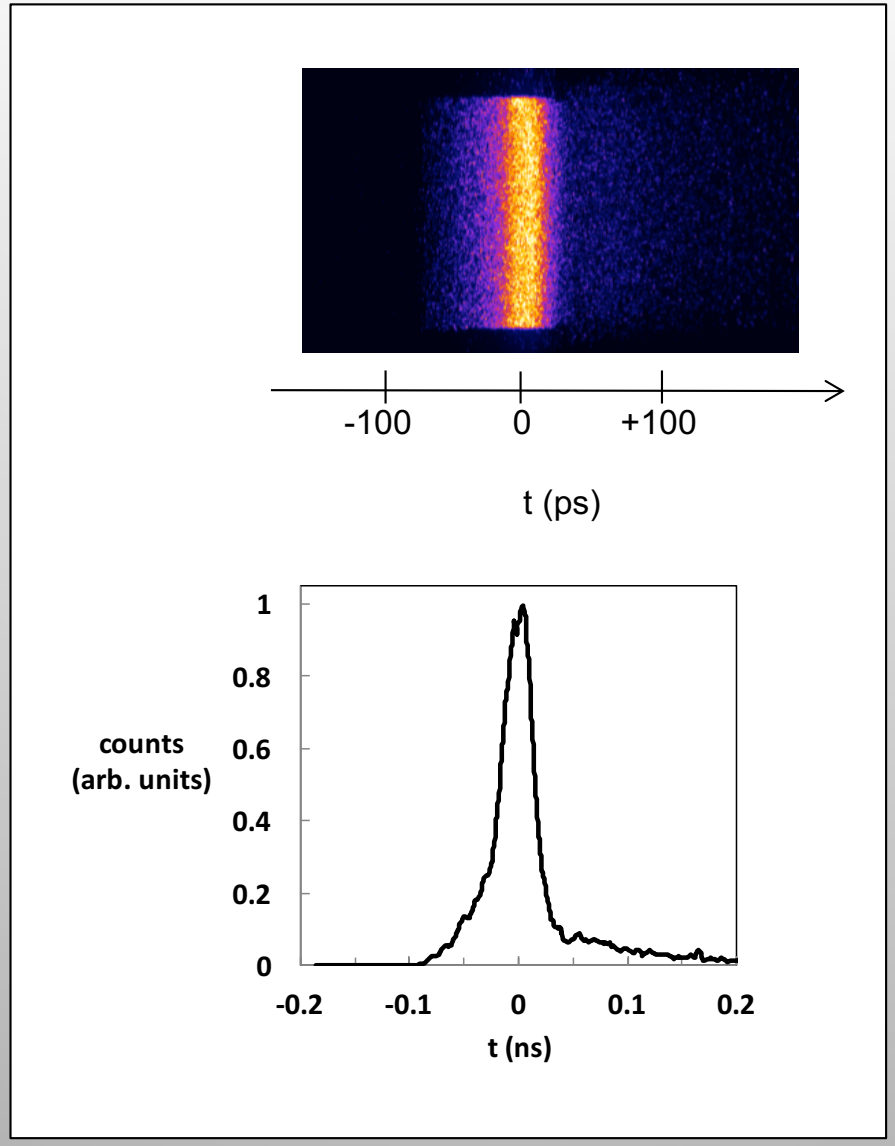

R Tommasini,et al.,PoP, 2017

Measuring source size: knife edge

Radiograph of a perfect knife edge

source

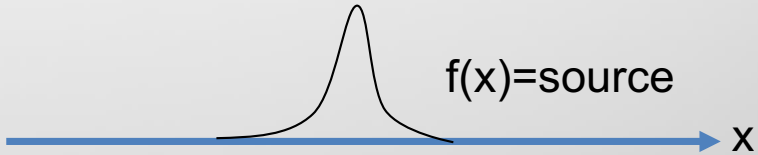

Knife edge

$$T(x) = \begin{cases} 1, x < 0 \\ 0, x \geq 0 \end{cases}$$

Radiograph

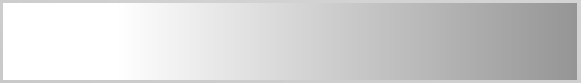

$$R(x) = \int_{-\infty}^{+\infty} f(t)T(x-t)dt = \int_{-\infty}^{x} f(t)dt$$

Ignoring noise: the source is given by the derivative of the radiograph:

$$f(x) = \frac{dR(x)}{dx}$$

Reconstructing the source: spherical imager

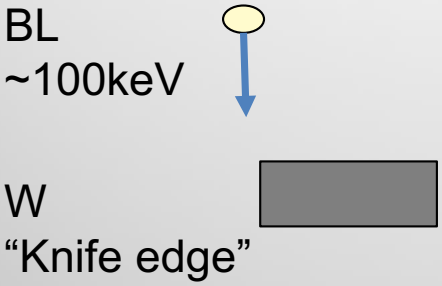

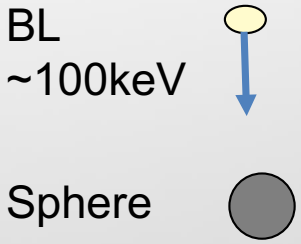

Simple but not practical:

- For 100-200keV X-rays there's no knife edge. E.g. W has to be ~1cm thick: parallax and tilt will affect the measurement
- Would reconstruct the source only wrt one direction

- Transmission is analytical:

$$s(r) = \begin{cases} e^{-2\kappa\varrho\sqrt{R^2-r^2}}, r < R \\ 1 \qquad\qquad\qquad\quad , r \geq R \end{cases}$$

- R = f ∗ s: f by deconvolution

- Does not require alignment
- Allows source reconstruction in all directions (2D)

R Tommasini,et al.,PoP, 2017

Backlighter source size ~ wire diameter
High resolutions are achievable with small wires

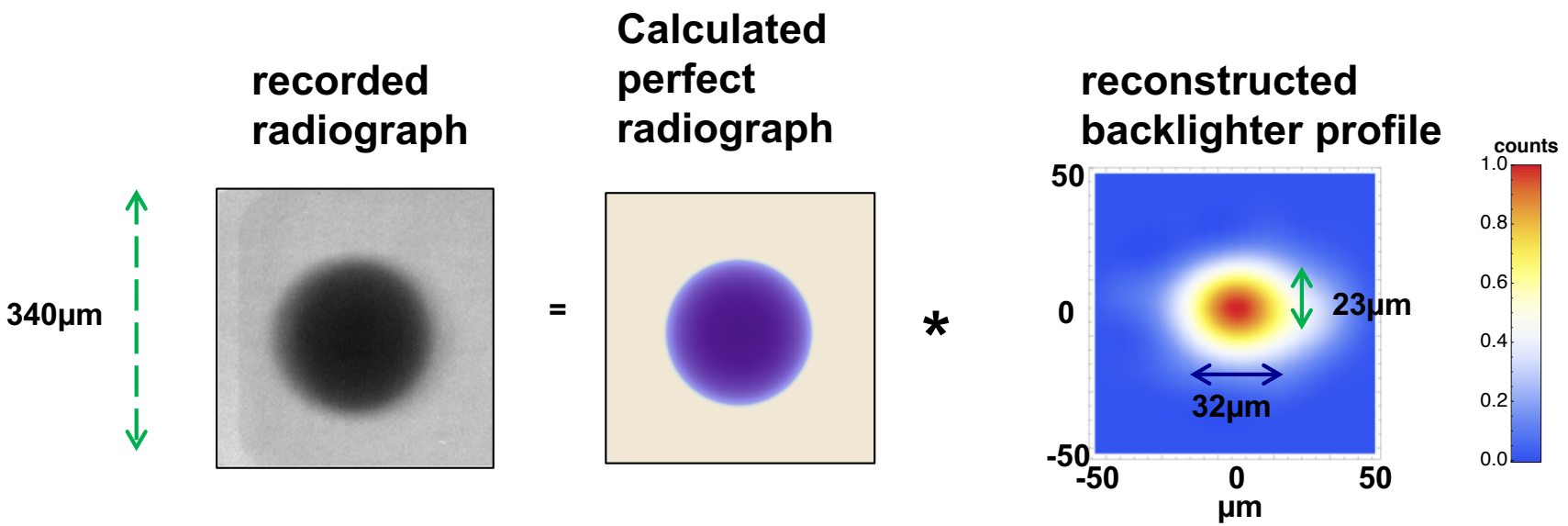

A sphere is a perfect test object and does not require alignment (as opposed to knife edges).
The "sphere imager" allows the reconstruction of the BL by deconvolution of calculated WC sphere radiograph

R Tommasini,et al.,PoP, 2017

Consistency check shows excellent agreement

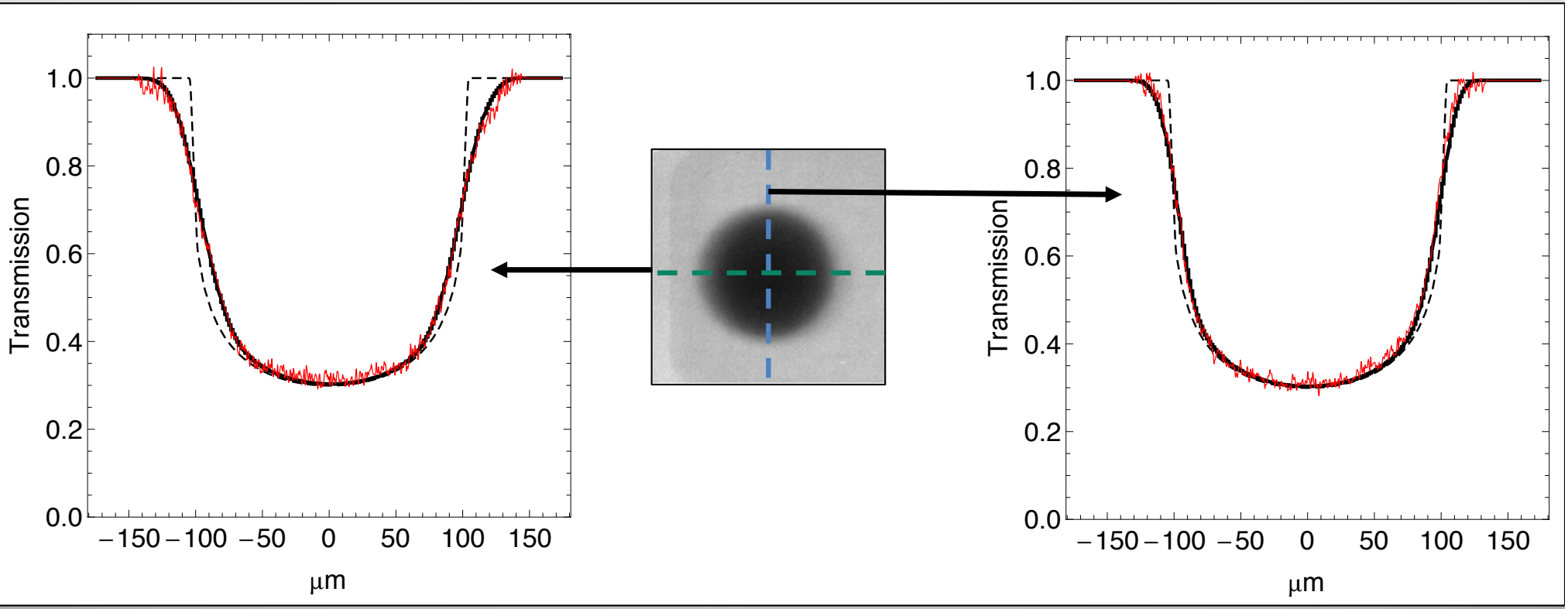

convolve reconstructed backlighter with calculated radiograph of sphere and compare with data

R Tommasini,et al.,PoP, 2017

Outlook

Motivation

- Our problem: probing ICF targets
- This requires the use of X-rays
- Plasmas are efficient sources of X-rays

Summary

- What is ICF
- Need to image ICF targets
- Laboratory-generated X-ray sources: laser plasma
  - Basic Plasma parameters
  - Basics of Radiation emission from laser-plasmas
- Imaging techniques
- Development of fast X-ray backlighters for ICF
- Application of Radiography to ICF targets

What information can we extract from X-ray radiographs ?

- **Fuel shape information**
- **Density, ρ, from reconstruction techniques**
- **Measurements of areal density, ρR, which is fundamental parameter to achieve ignition**

The ultimate goal is the reconstruction of the density starting from projections: Unfold

In this particular case, the projection is the 'transparency' provided by radiography.

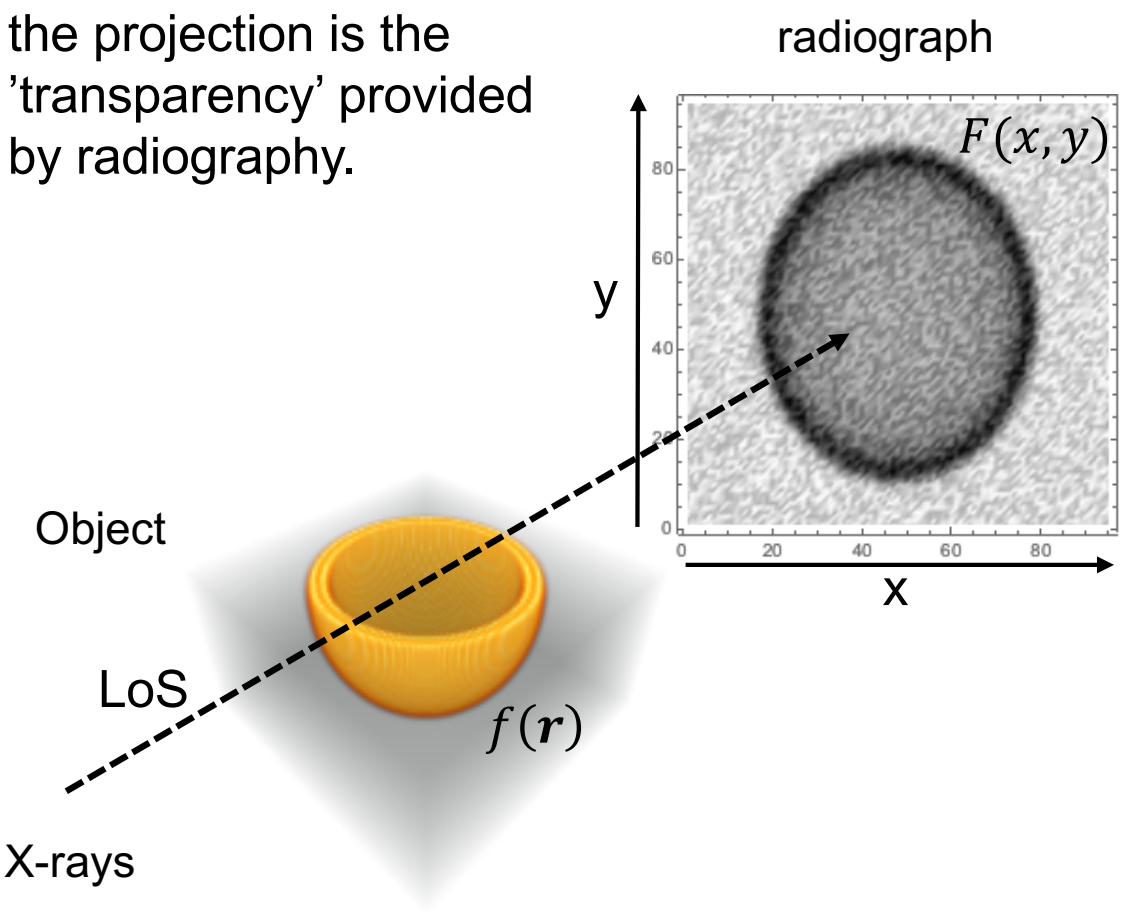

Task: Reconstruct density distribution of objects from radiographs or self emission images

Emission image	$I(x,y) = \int \varepsilon \, \varrho \, dl$
Radiograph	$\mathrm{T}(x,y) = e^{-\int k \, \varrho \, dl}$

In both cases we have to find f:

$$\int f(\boldsymbol{r}) dl = F(x,y)$$

Issue:
One single line of sight

For axially symmetric distribution Abel Inversion is the common approach

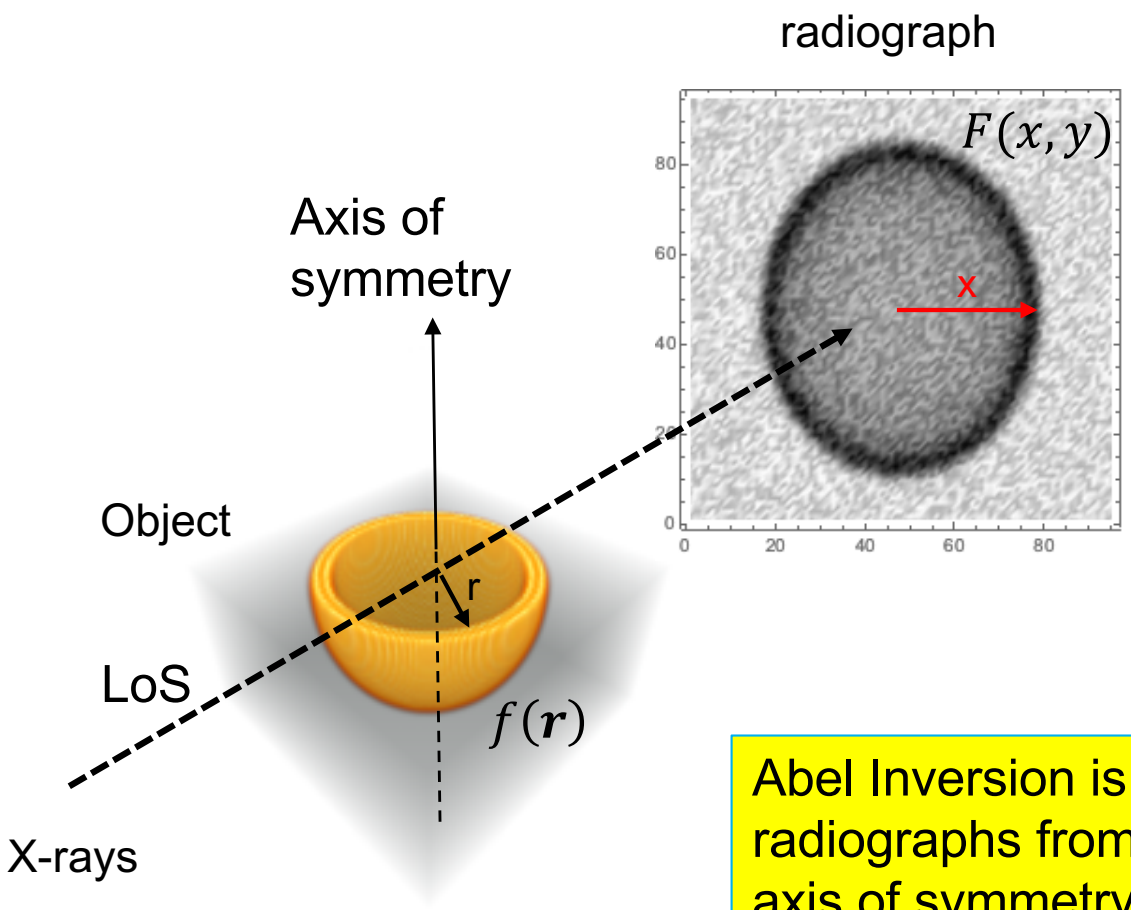

Abel Transform: $f(\boldsymbol{r}) \rightarrow F(x,y)$

$$F(x) = 2\int_x^\infty \frac{r\, f(r)}{(r^2 - x^2)^{1/2}}\, dr$$

Abel Inversion: $F(x,y) \rightarrow f(\boldsymbol{r})$

$$f(r) = \int_r^\infty \frac{-\frac{dF}{dx}}{\pi(x^2 - r^2)^{1/2}}\, dx$$

Abel Inversion is equivalent to assuming that radiographs from any LoS perpendicular to the axis of symmetry are the same: **prior knowledge**

Unfold from single LoS is a ill-posed problem

Well-posed problems obey the following criteria (J. Hadamard, 1923)

1. The problem must have a solution
2. The solution must be unique
3. The solution must be stable under small changes to the data

Unfold from single line of sight projection is ill-posed problem: violates 2

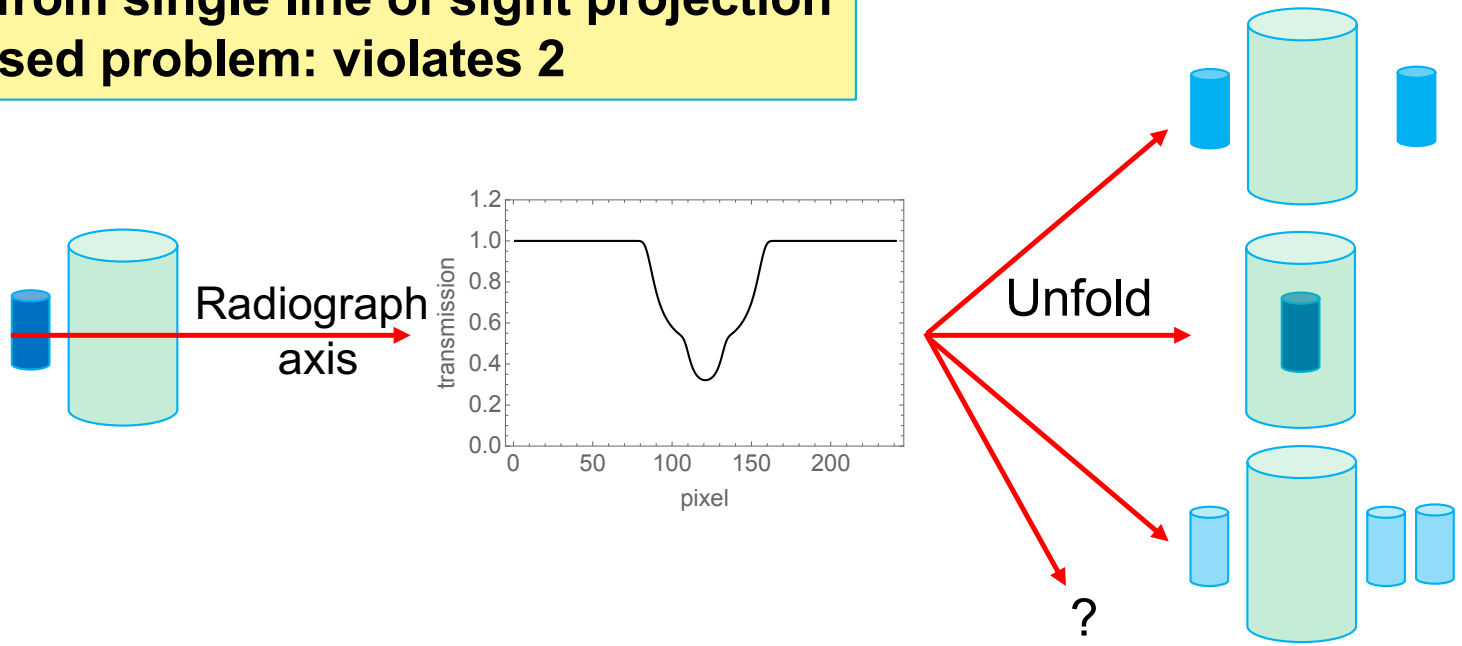

Numerical Abel Inversion also violates 3

Numerical Abel inversion amplifies noise into large errors in the deconvolved density distribution. I.e. it is not stable under small changes to the data

Test case: Noisy Radiograph of shell

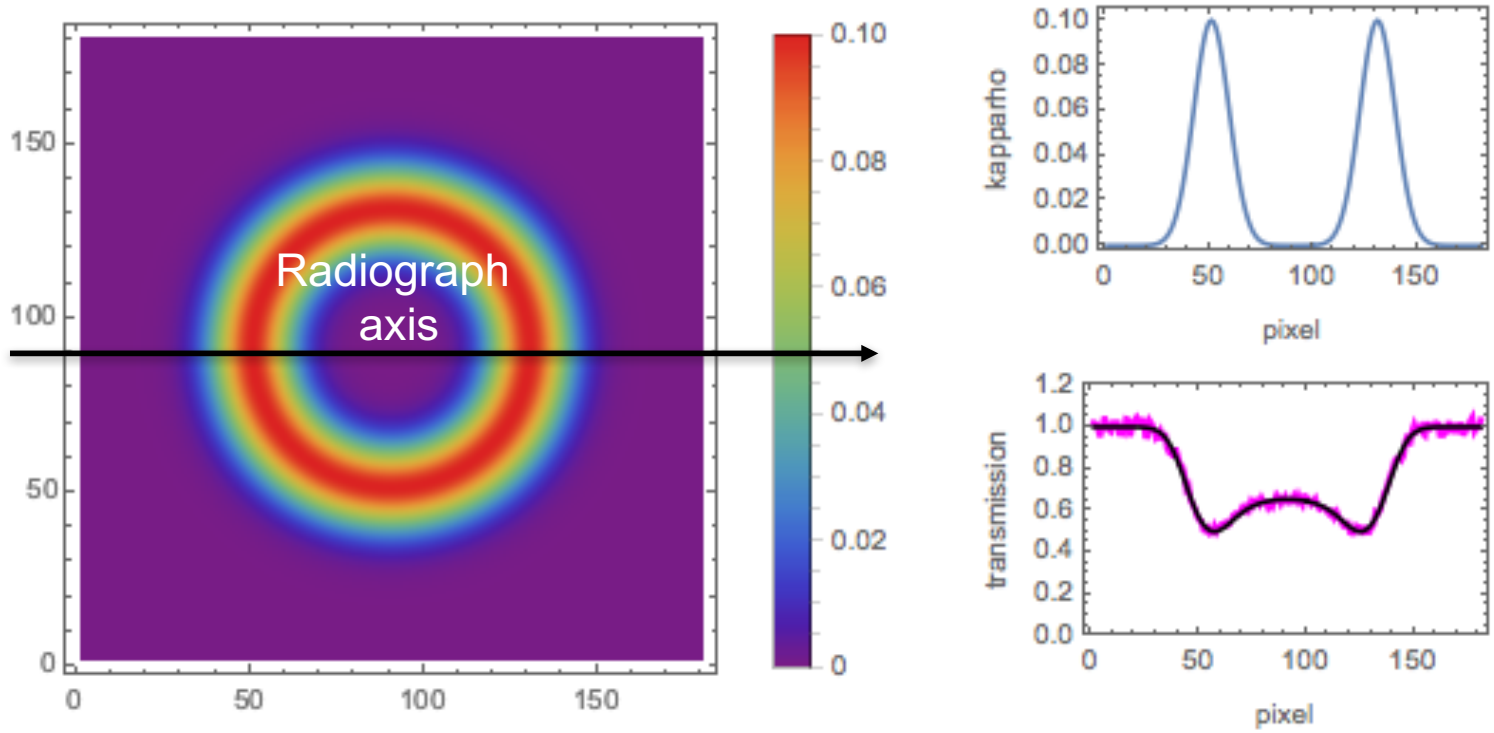

Numerical Abel Inversion also violates 3: noise is largely amplified

Noise increase is nonlinear

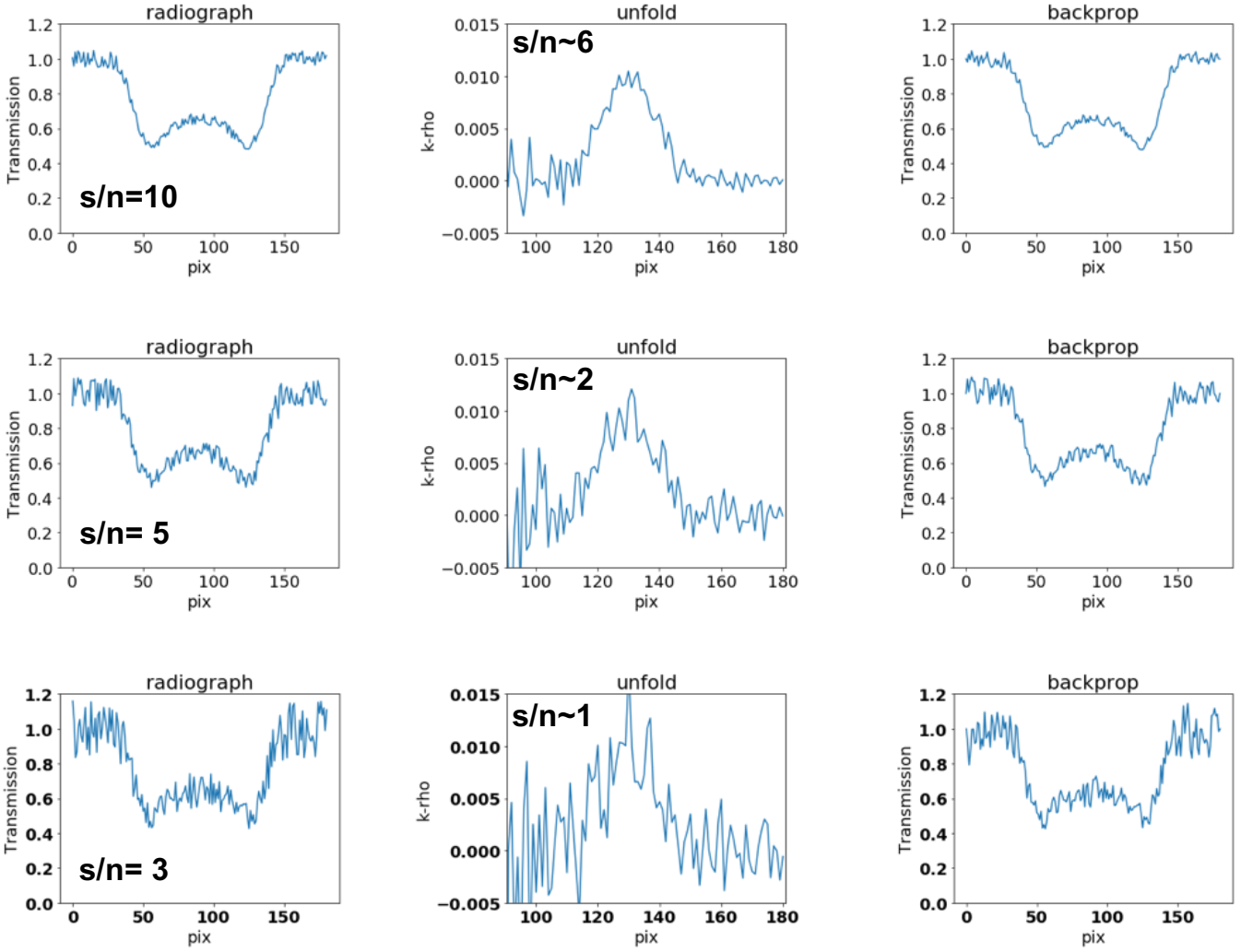

Abel Inversion can't handle asymmetric radiographs

k-rho model: slice = central

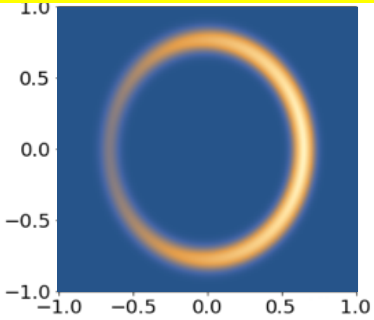

radiograph

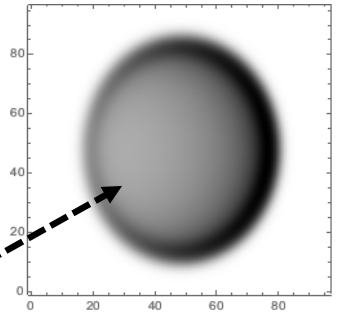

Object

X-ray

Abel Inversion: slice = ?

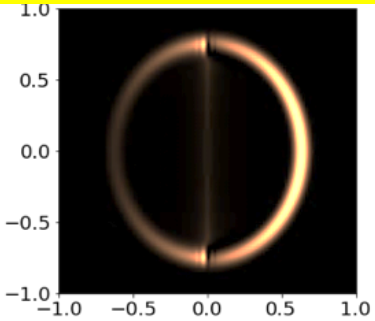

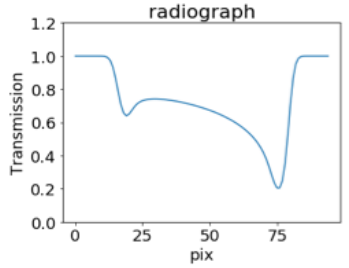

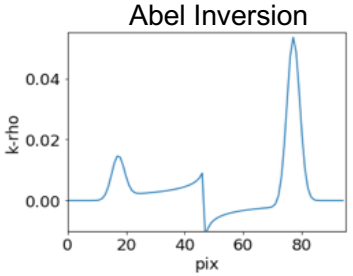

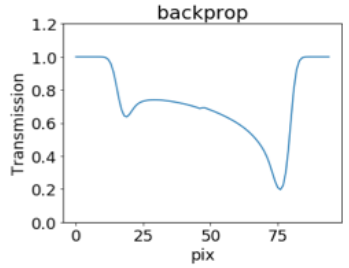

Negative values for density are allowed

Some can be mitigated. E.g. separated Left-Right inversions… However one has to handle merging of the two halves.

Unfold can be done based on forward fit

a) A 3D density distribution is defined on a cylindrical grid
   - Still needed as only one LoS

b) Front-Rear symmetric density is allowed to change wrt the azimuthal and polar angles
   - Relax cylindrical symmetry

c) The density is reconstructed by fitting its radiograph or image to the data
   - no Abel Inversion: robust to noise

- Constraints are easily imposed: e.g., non-negative density

- Due to single line of sight, introduction of some form of **prior knowledge** is unavoidable. In this case the cylindrical grid
- In the next VGs: Unfold code put to test

Single ring test cases: geometry

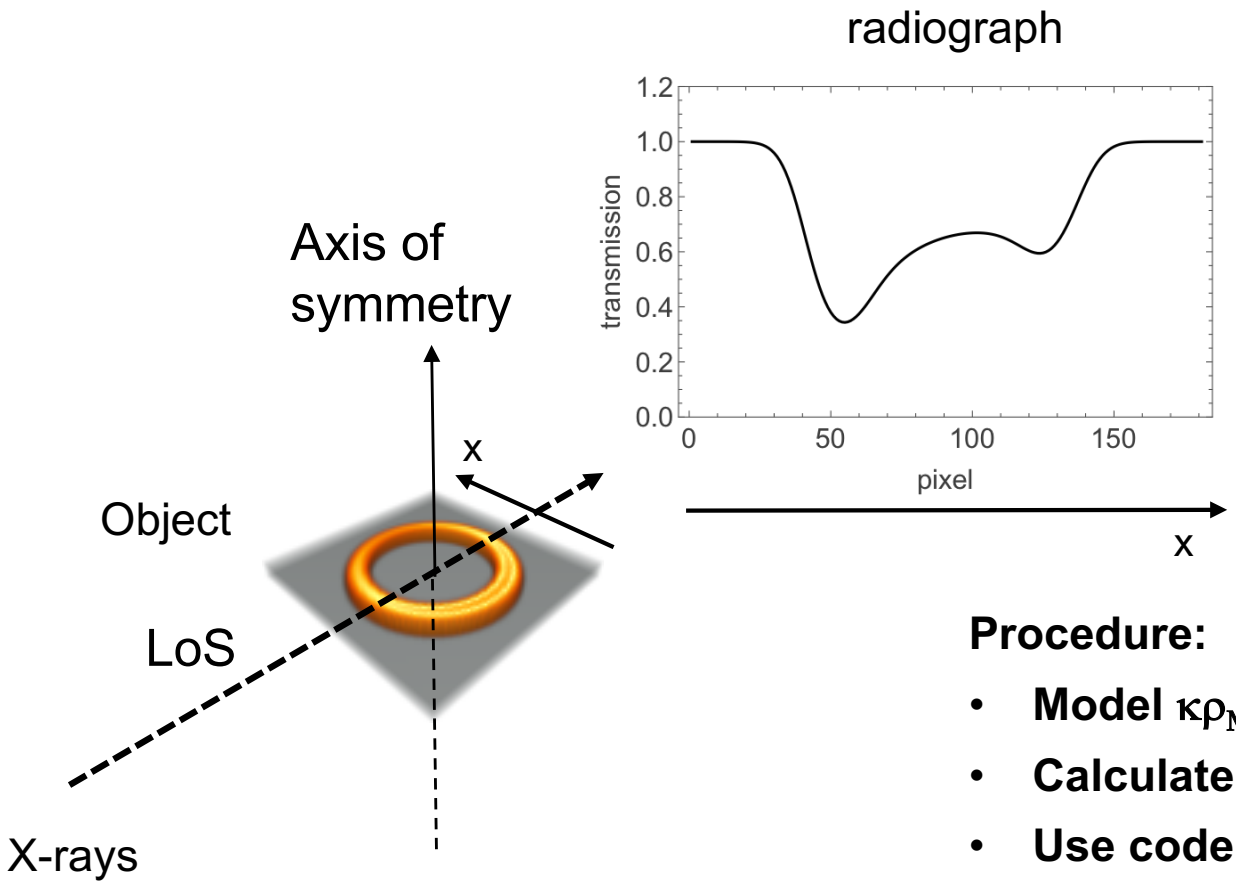

Procedure:

- **Model $\kappa\rho_M$ distribution**
- **Calculate radiograph**
- **Use code to unfold $\kappa\rho$ from radiograph**
- **Compare $\kappa\rho$ and $\kappa\rho_M$**
- **Compare radiographs from $\kappa\rho$ and $\kappa\rho_M$ (propagation test)**

Asymmetric density distribution ring

Model

Radiograph axis

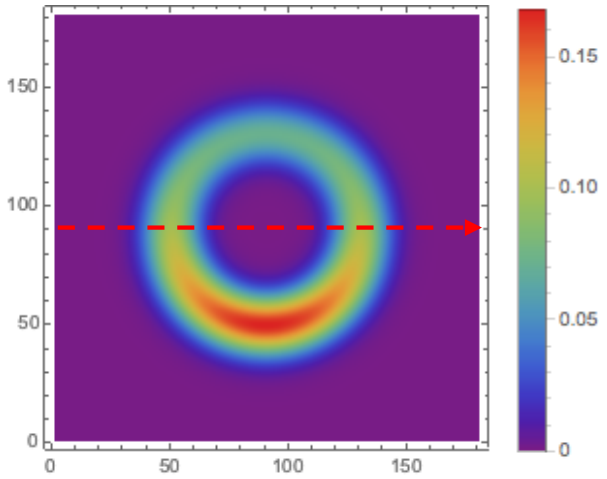

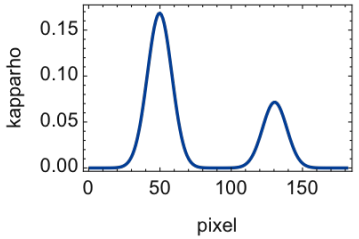

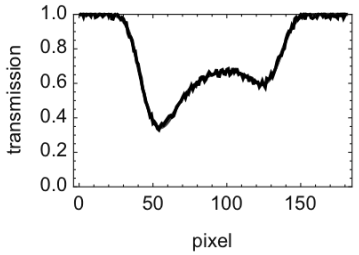

Top view

Unfold

Radiograph axis

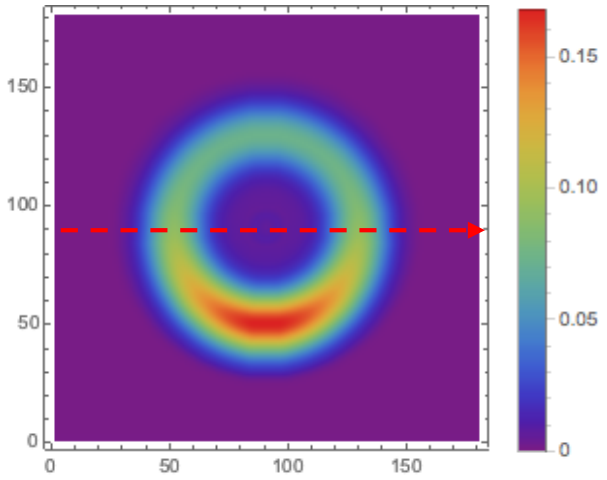

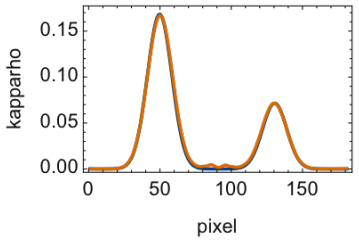

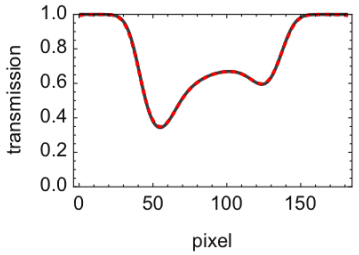

propagation test

Asymmetric density distribution: nested rings

Model

Radiograph axis

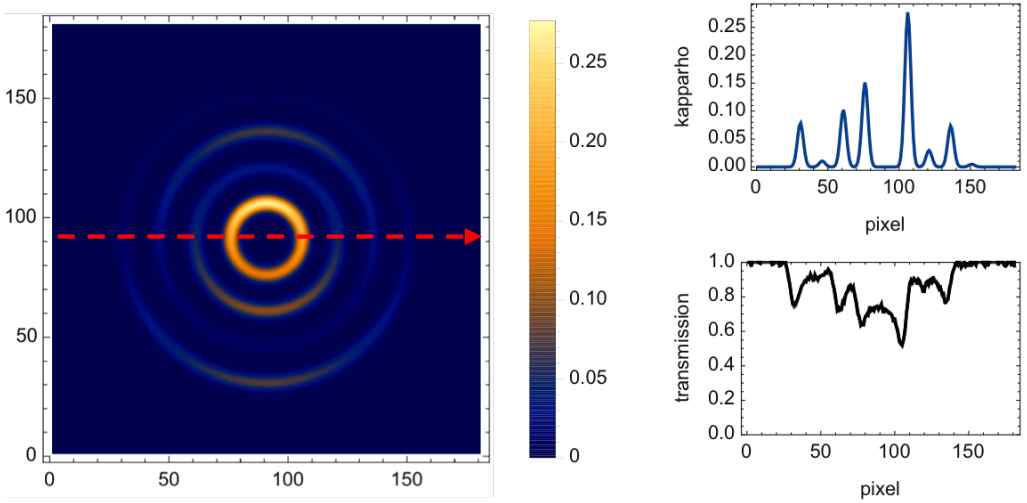

Top view

Unfold

Radiograph axis

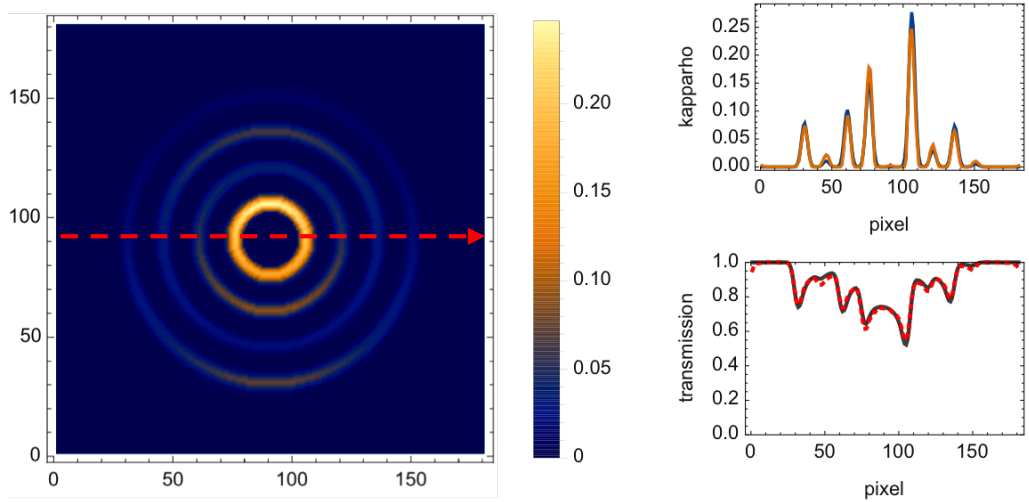

propagation test

The unfold problem still violates uniqueness of solution However the code is very stable wrt noise

Well-posed problems obey the following criteria (J. Hadamard, 1923)

1. The problem must have a solution
2. **The solution must be unique: It isn't**
3. **The solution must be stable under small changes to the data: It is**

Unfold from single line of sight, image or radiograph, is ill-posed problem: violates 2.

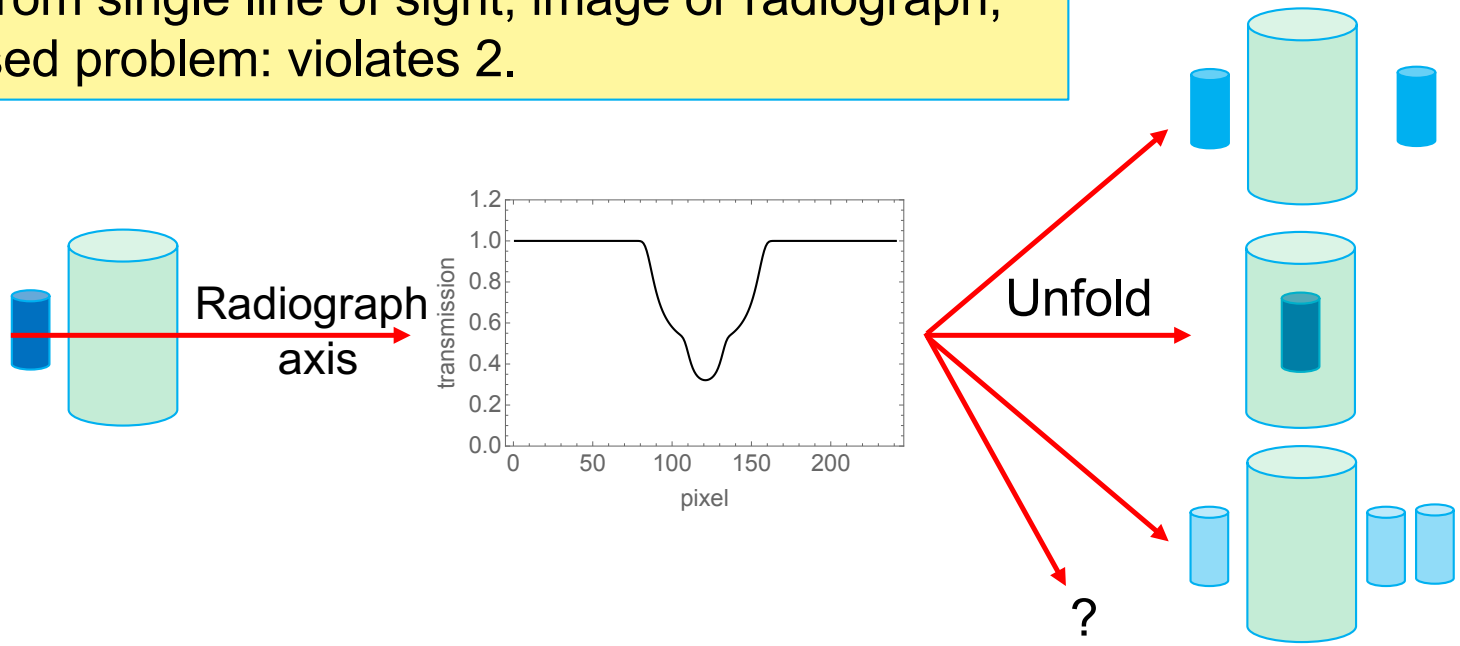

Degeneracy: single LoS degeneracy

Model

Radiograph axis

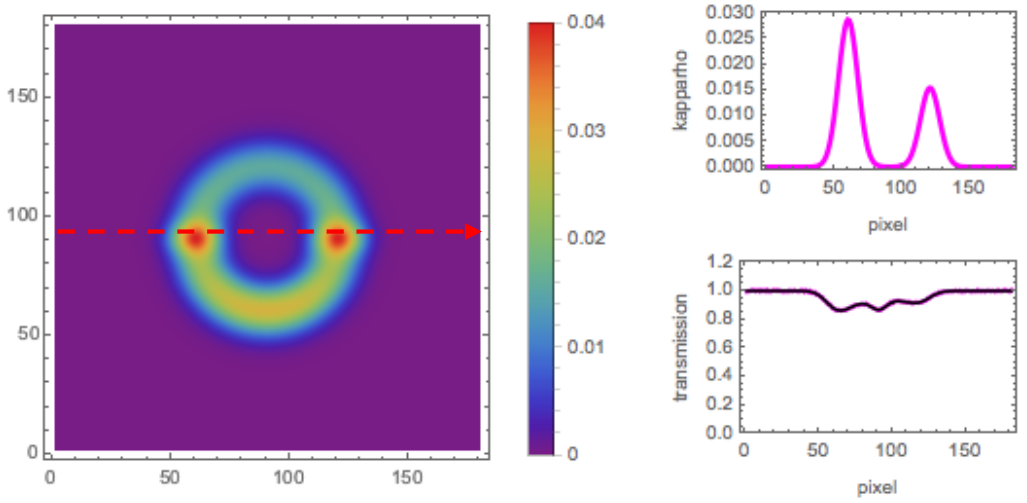

Top view

Unfold

Radiograph axis

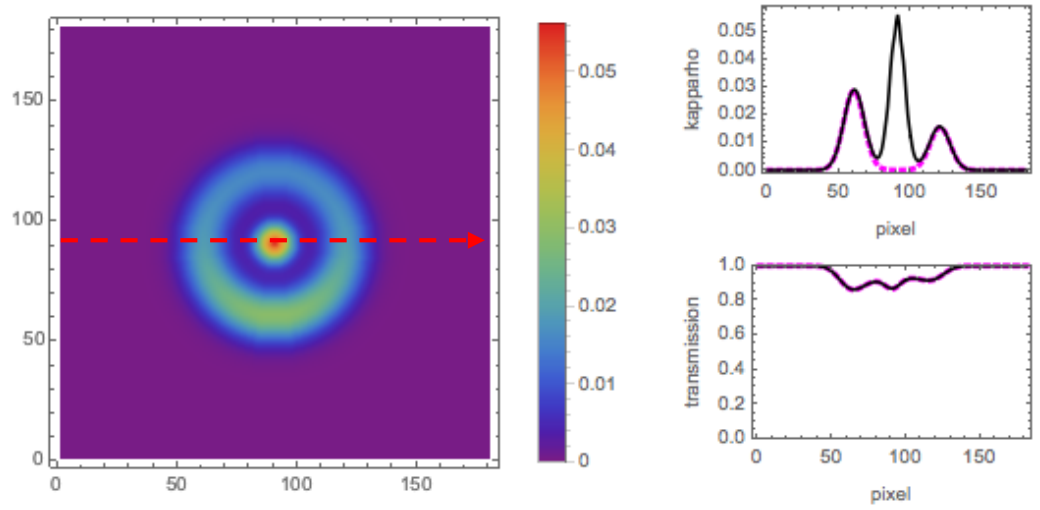

Due to single LoS, the code places density in the center

propagation test

Degeneracy: 45 deg rotation wrt single LoS. We cannot correctly reconstruct asymmetries with component along the LoS

Model

Radiograph axis

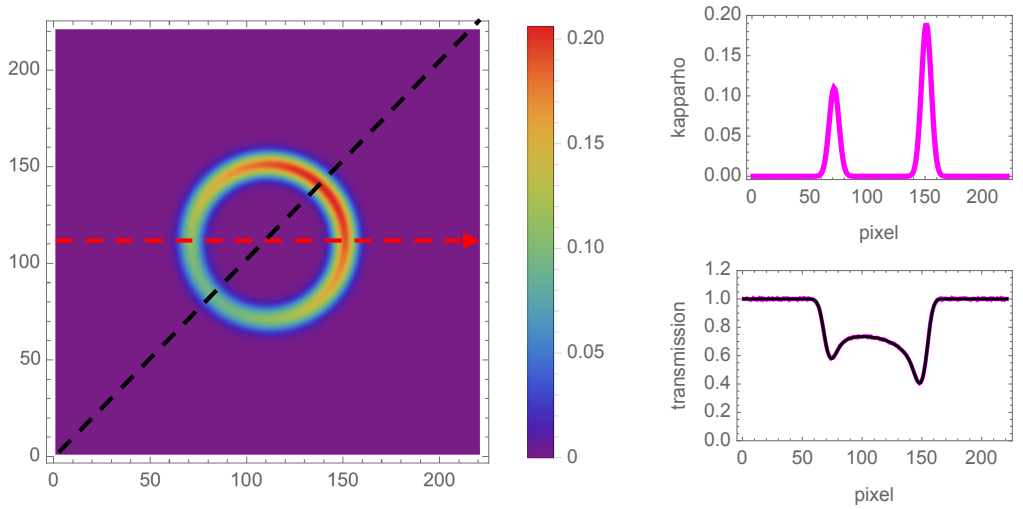

Top view

Unfold

Radiograph axis

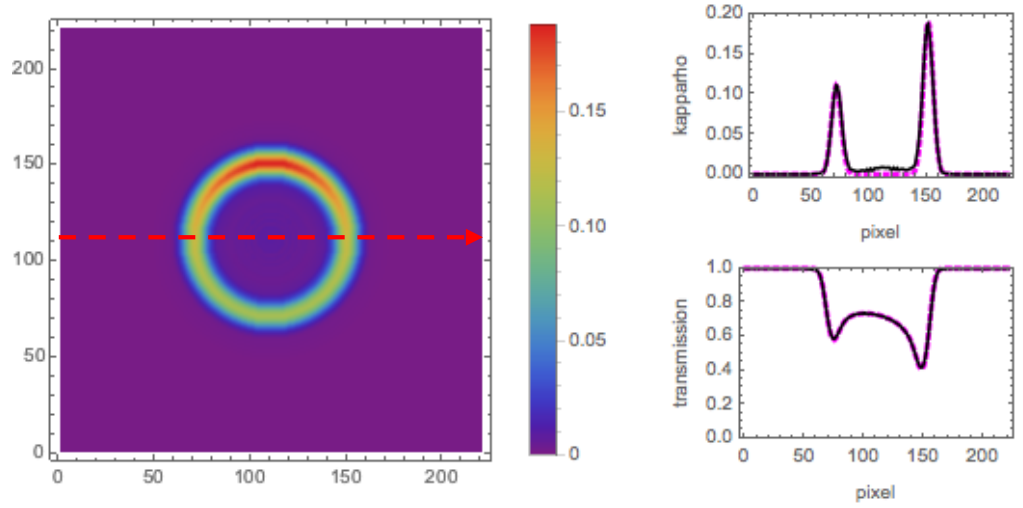

The code finds the only possible solution compatible with single LoS

propagation test

However the code is very stable wrt noise

Radiograph S/N

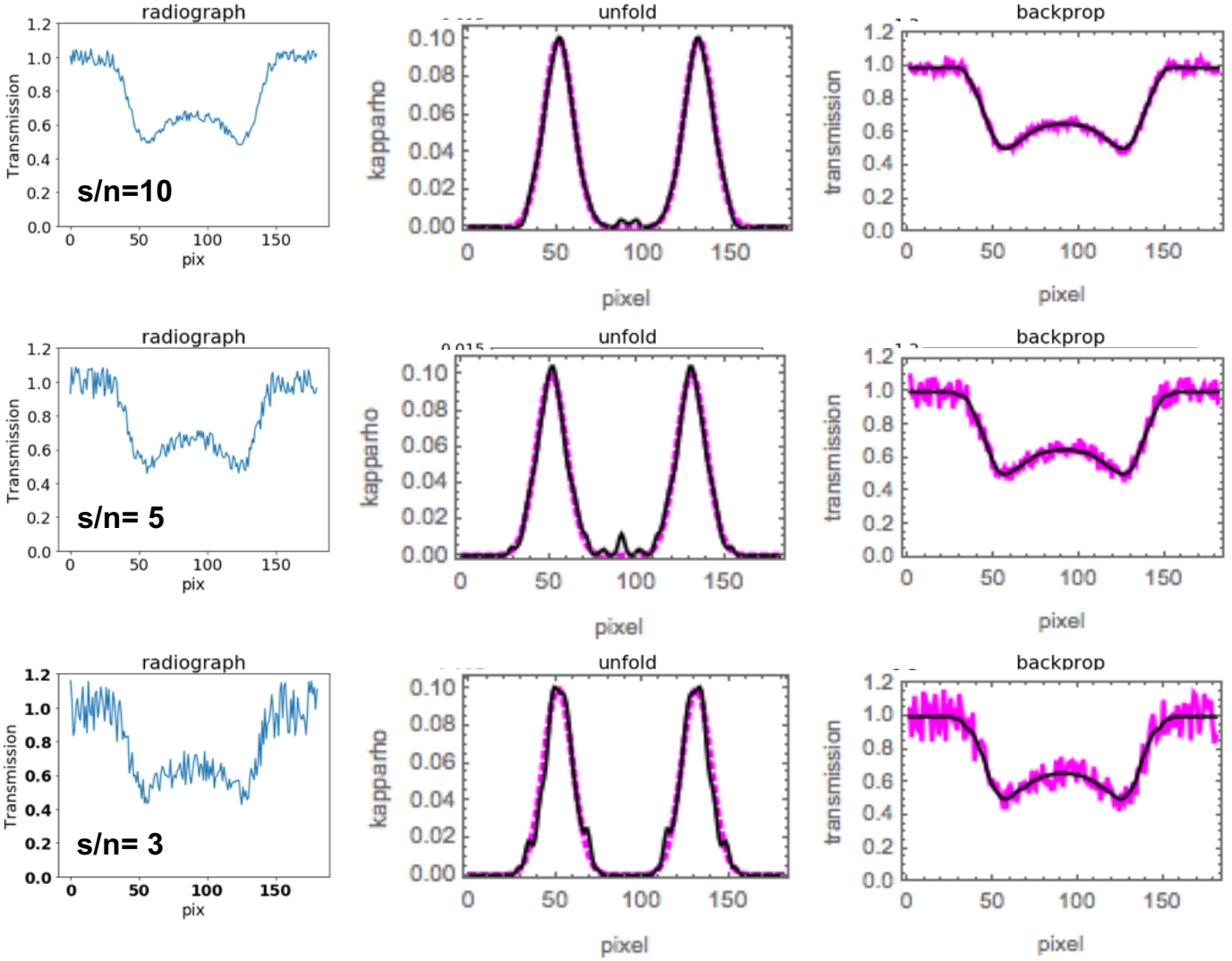

Test on 2D radiographs

Simulated Asymmetric density distribution

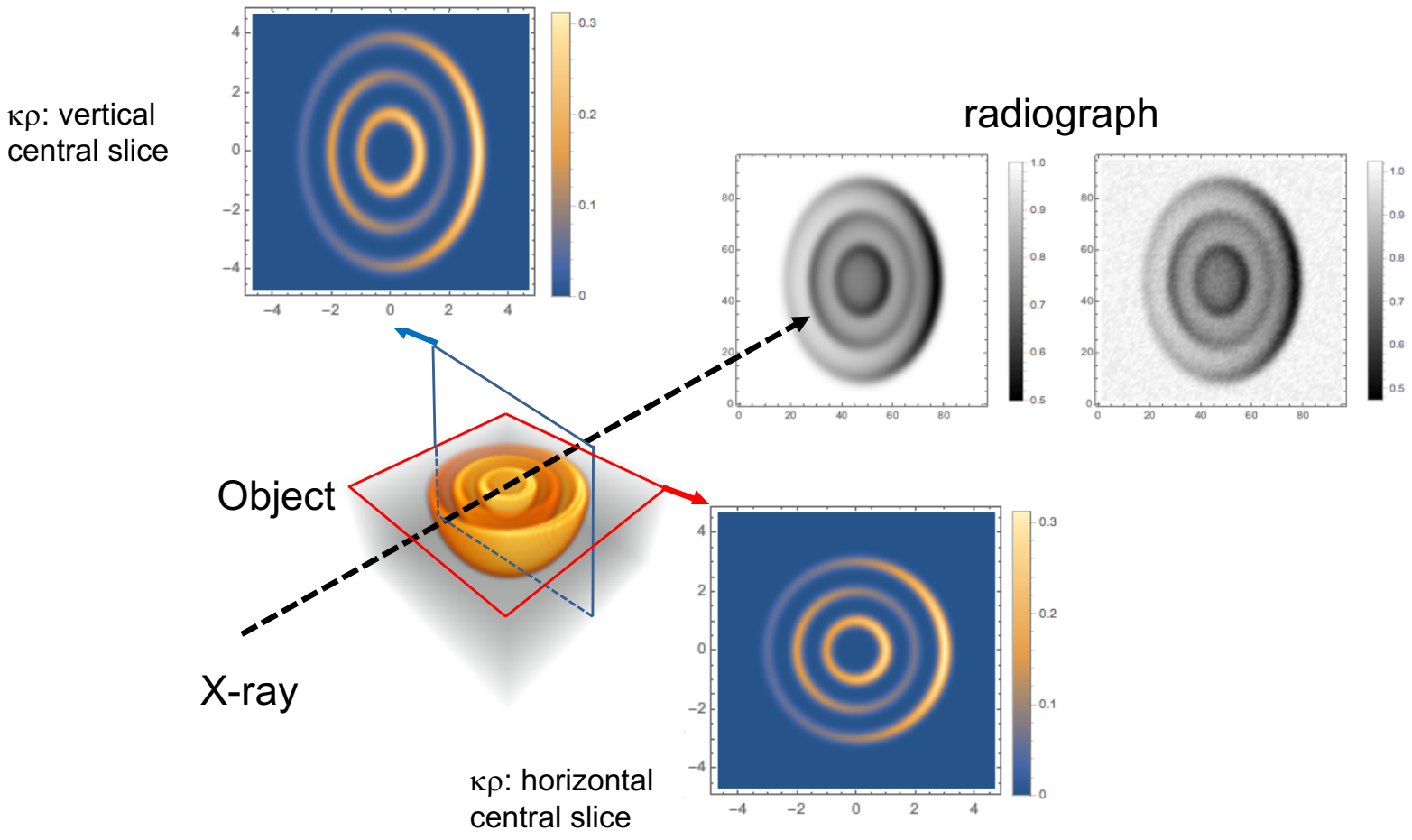

Single LoS 2D radiograph -> “3D” object reconstruction

Model κρ

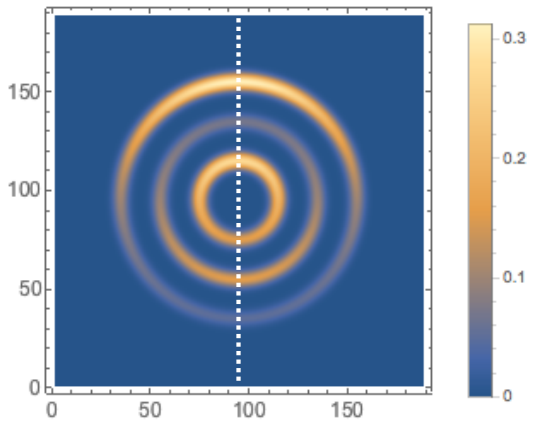

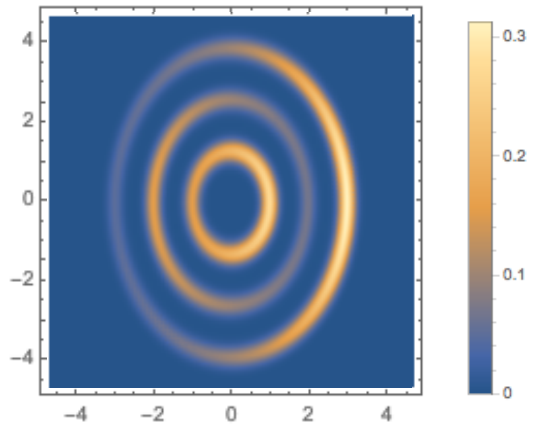

κρ and transmission lineout comparison

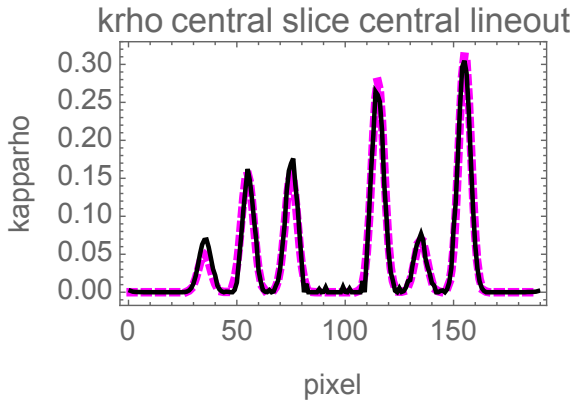

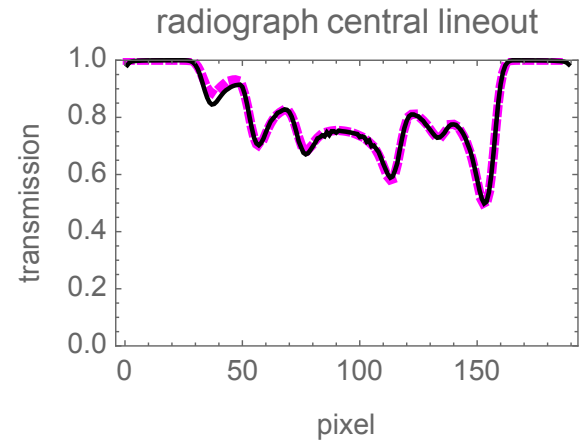

Reconstructed κρ

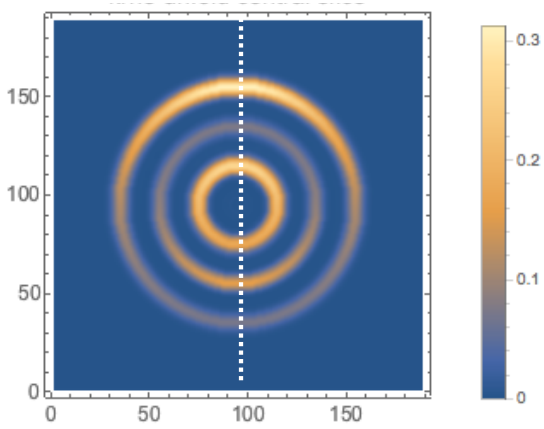

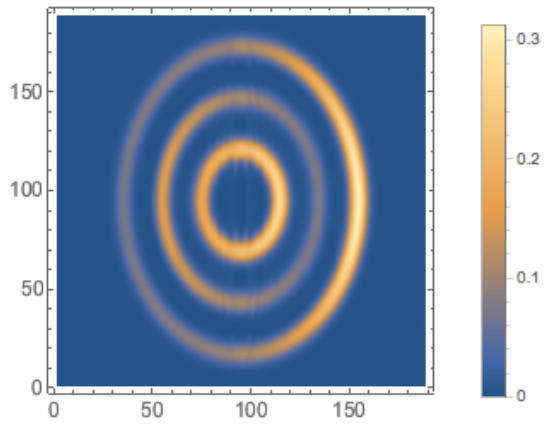

Single LoS 2D radiograph -> “3D” object tomography

Model $\kappa\rho$

Reconstructed $\kappa\rho$

Reconstruction of small, sharp defects: tent

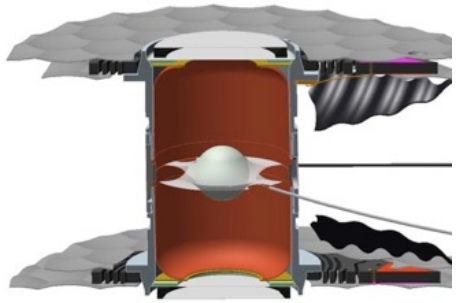

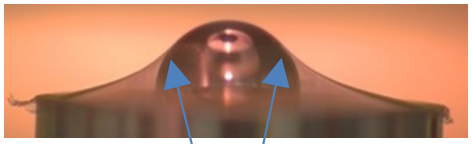

RT growth is seeded where support tent leaves capsule

HF shot, 45nm tent

radiograph

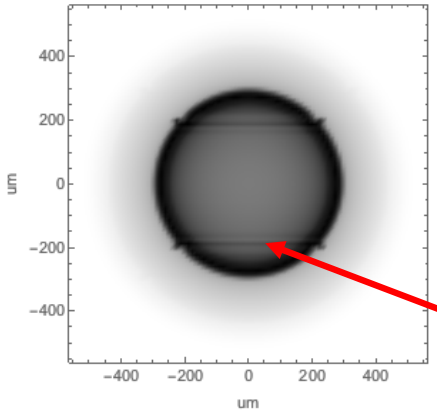

Unfold →

Tent-induced scar

Reconstructed Density map
arb units

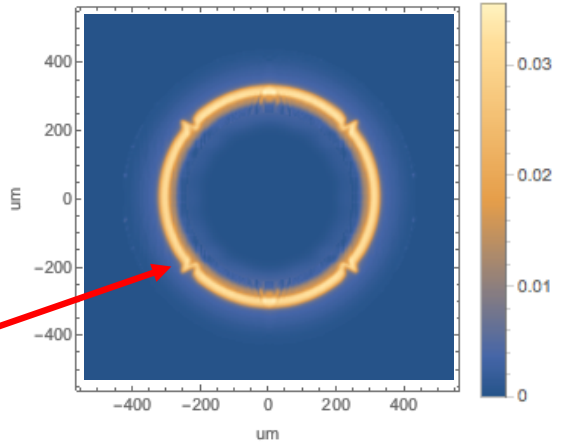

Radiograph simulation by *B. Hammel*

Code works well on reconstruction of small, sharp defects: tent

Reconstructed Density map

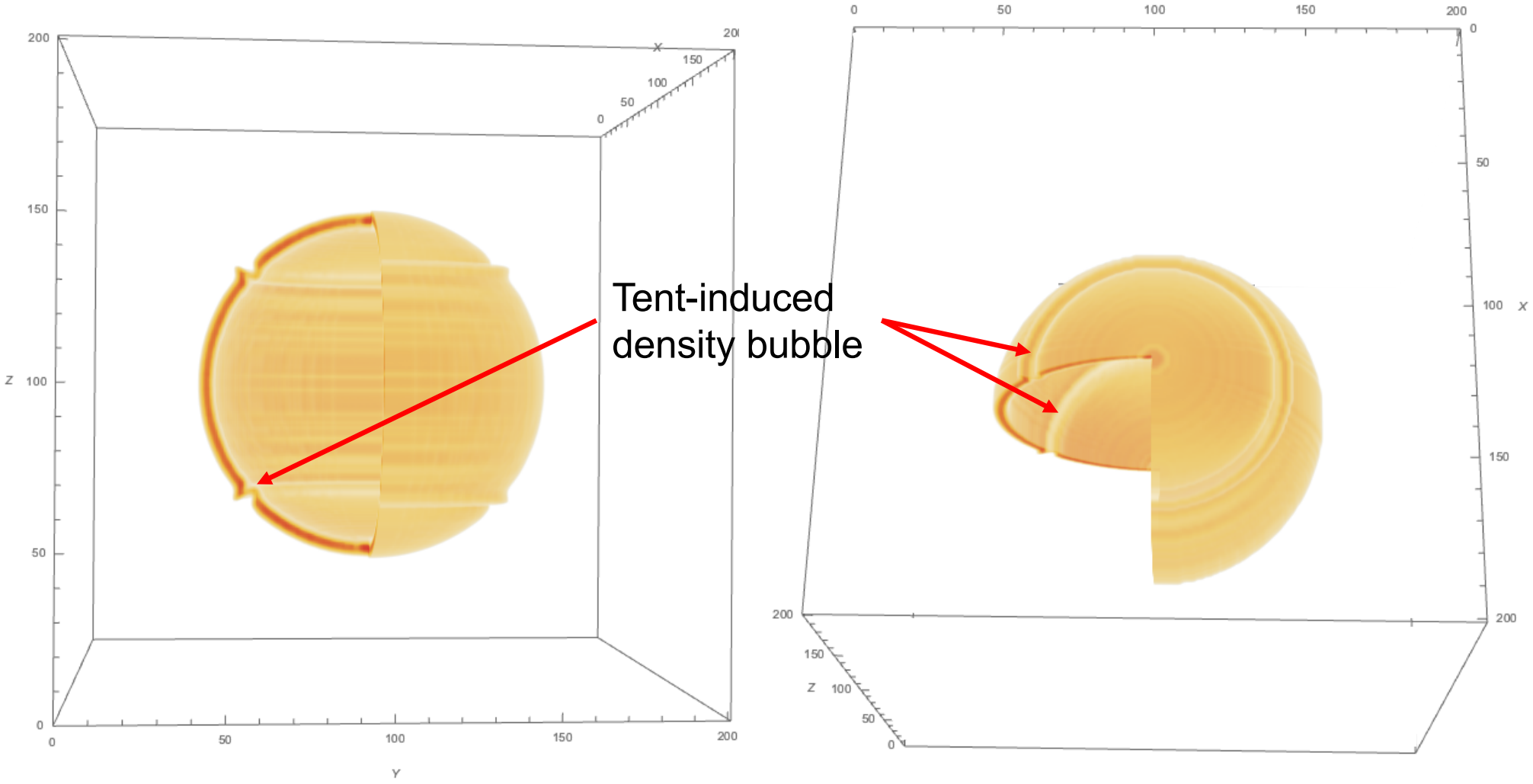

Unfold of 2D radiographs has shown that a tent, just 110 nm thick, can substantially perturb an implosion

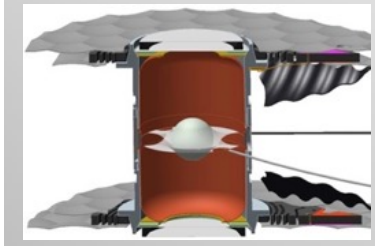

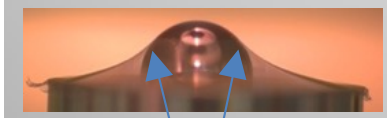

Contact points: tent-capsule

10keV Radiograph at ~630ps prior to peak compression

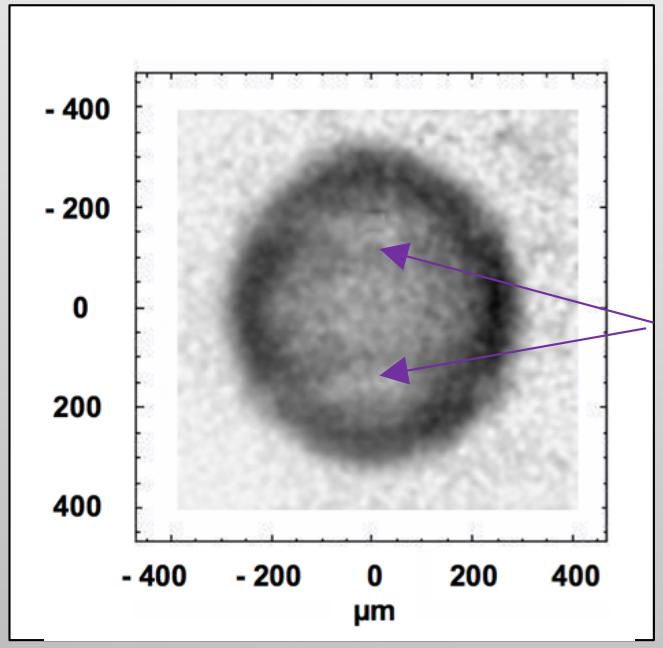

RT-grown tent induced scars

Reconstruction of capsule density

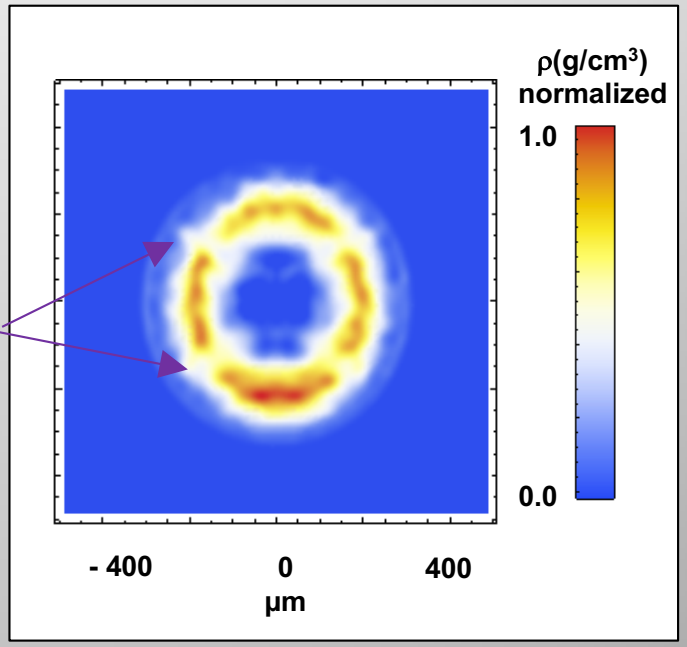

Δ(ρR)/ρR~20% at tent locations

PoP 22, 056315 (2015).

2D radiographs show scars on imploding capsule seeded by tent contact points

10keV Radiograph at ~630ps prior to peak compression

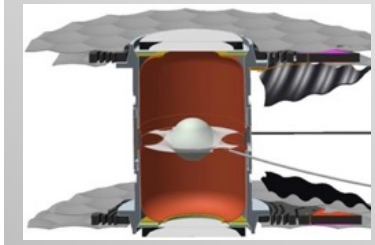

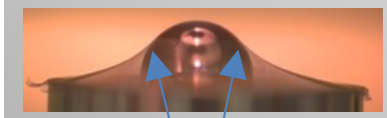

Contact points: tent-capsule

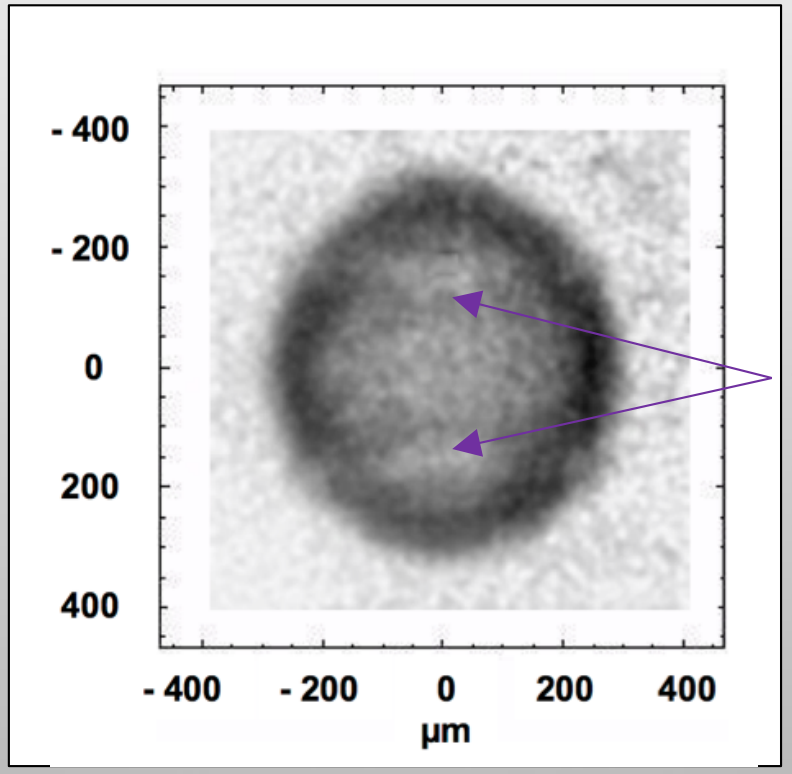

RT-amplified tent induced scars

PoP 22, 056315 (2015).

Unfold of 2D radiographs has shown that a tent, just 110 nm thick, can substantially perturb an implosion

Reconstruction of capsule density by Unfold

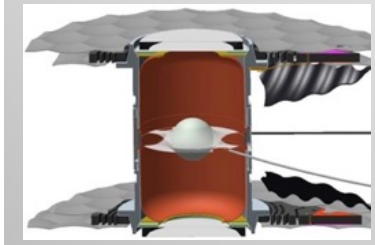

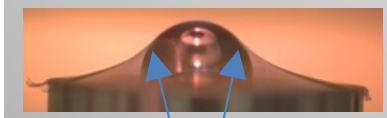

Contact points: tent-capsule

4-fold density bubble seeded by tent

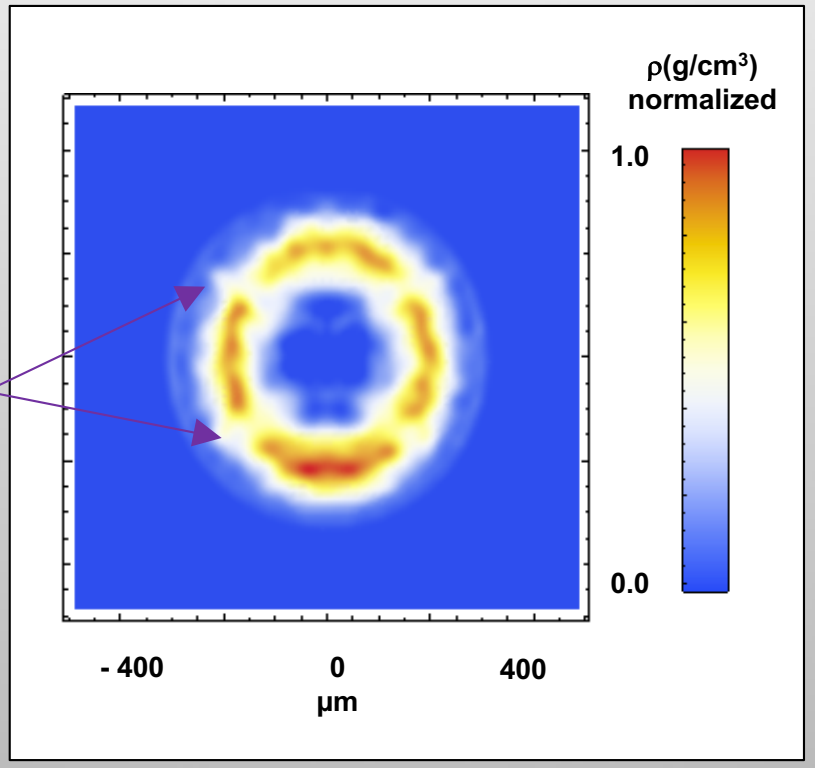

Δ(ρR)/ρR~20% at tent locations

PoP 22, 056315 (2015).

Data show linear degradation of the normalized yield as the fractional Δ(ρR)/ρR increases above about 5%

Y_n^* is normalized to properly compare implosions using hohlraums with different lengths, Laser Entrance Hole diameters, and gas fills.

Yields are reduced as much as 2.3x when Δ(ρR)/ρR ~ 20%

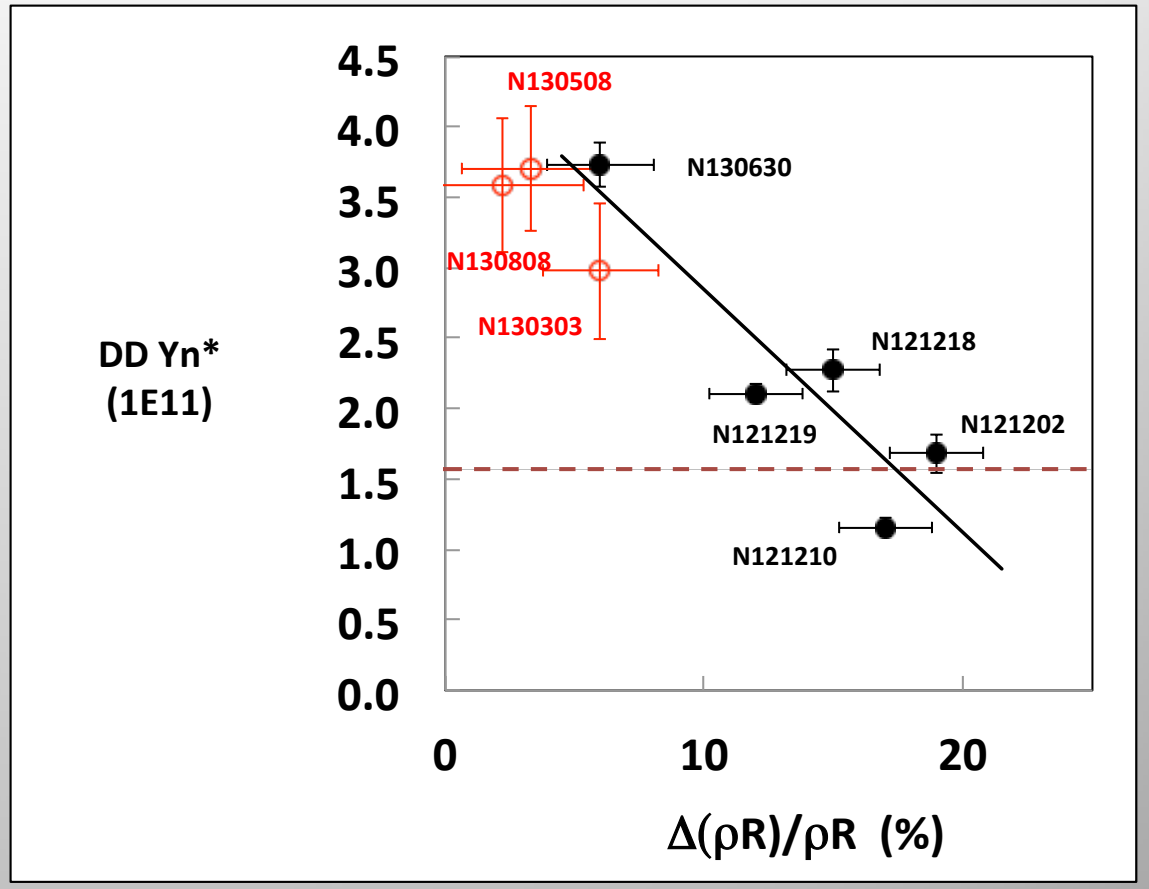

PoP 22, 056315 (2015).

Summary

- X-ray Imaging of ICF targets is paramount to
  - Understand reasons for failures
  - Optimize experiments
- Laser-plasmas are ideal X-ray sources
- The main Imaging techniques for the fuel are based on backlighting
- Application: 2D gated radiographs to measure growth of ρR perturbations seeded by the capsule support tent in ICF hohlraums at the NIF

Thank you!

Lawrence Livermore
National Laboratory